



THE UNIVERSITY OF
WAIKATO
Te Whare Wānanga o Waikato

Research Commons

<http://researchcommons.waikato.ac.nz/>

Research Commons at the University of Waikato

Copyright Statement:

The digital copy of this thesis is protected by the Copyright Act 1994 (New Zealand).

The thesis may be consulted by you, provided you comply with the provisions of the Act and the following conditions of use:

- Any use you make of these documents or images must be for research or private study purposes only, and you may not make them available to any other person.
- Authors control the copyright of their thesis. You will recognise the author's right to be identified as the author of the thesis, and due acknowledgement will be made to the author where appropriate.
- You will obtain the author's permission before publishing any material from the thesis.

Instrumentation of Environment Lab Filter Columns, Settling Tanks and Flocculators

A thesis submitted in partial fulfilment
of the requirements for the degree of

Master of Engineering

by

Weiyang Luo



THE UNIVERSITY OF
WAIKATO
Te Whare Wānanga o Waikato

Hamilton, New Zealand

March 2021

Abstract

This project was focused on the installation of three water purification systems in the environmental lab of the University of Waikato. Each system consists of a flocculator, a settling tank (clarifier) and a filtration column. The settling tanks were different from each other, one conventional, one laminar and one hopper-bottom clarifier.

The systems were then to be linked with instrumentation to measure and control the purification process in Arduino. The instrumentation included

- One flowmeter
- Two pH meters
- Two Turbidity sensors
- One zeta potential meter

Turbidity meters at the inlet to the coagulation and flocculation system, after the coagulation and flocculation, after the clarifiers and after the filters.

The instrumentation was also required to log their reading so students could collect and analyse the data.

The instruments required for the project were purchased with a budget. Prior to the purchase, a list of all items to be purchased was made with comparison on the specification as well as the price.

A P&ID diagram was made showing the schematic relations between instruments and the equipment.

Once installation of the system was complete, calibration of the sensors were conducted before the runs of the system, whereupon data was collected and analysed.

Acknowledgements

I would like to thank Doctor Mark Lay of the Engineering Department of the University of Waikato, who guided me patiently through this research process and provided me guidelines of my thesis structure.

A thank you to Doctor Graham Glasgow and Peter Kovalsky as well for giving me advice and providing me with electronic components.

Dr Lisa Li inducted me along with other lab users on the regulations and guidelines of the environmental lab, a special thanks to her as well.

And thanks to all fellow students in the office, who never hesitated to lend me a helping hand whenever the occasion arose.

Mohammed Ibrahim A Almansaf helped me with the installation of the initial and final water treatment system. A special thanks to him.

Table of Contents

Acknowledgements.....	ii
Table of Contents.....	iii
List of Figures.....	vi
List of Tables.....	viii
1 Introduction.....	1
1.1 Overview.....	1
1.2 Problem Statement.....	2
1.3 Project Aims.....	2
1.4 Structure of the Thesis.....	2
2 Literature Review.....	5
2.1 Overview.....	5
2.2 Primary Screening.....	7
2.3 Coagulation and Flocculation.....	7
2.4 Static Mixers.....	12
2.5 Tank Mixing.....	14
2.5.1 Passive Systems.....	15
2.5.2 Agitators.....	16
2.6 Settling Tanks.....	22
2.6.1 Conventional Clarifier.....	23
2.6.2 Lamina Clarifier.....	24
2.6.3 Hopper Bottom Clarifier.....	26
2.6.4 Settling Theory.....	27
2.7 Filtration.....	29
2.7.1 Types of Filtration.....	29
2.7.2 Filtration Theory.....	30
2.7.3 Pressure Drop.....	30
2.8 Measurement Theory.....	32
2.8.1 Zeta Potential Measurement.....	32
2.8.2 Turbidity Measurement.....	33
2.9 Control Theory.....	34
2.10 Example of Lab-Scale Water Treatment for Teaching.....	36
2.11 A Case Study on Arduino for Teaching.....	37
3 Preparation Work on Electronic and Water Treatment Components.....	40

3.1	Theory and Preparation Work on Electronics	40
3.1.1	Motor Control	41
3.1.2	PH Sensor.....	42
3.1.3	Turbidity Sensor.....	43
3.1.4	Dosing Pump.....	45
3.1.5	Flowmeter	46
3.1.6	Zeta Potential Measurement	46
3.2	Water Treatment Components	47
3.2.1	Water treatment tanks	47
3.2.2	Filtration Column.....	49
3.2.3	Mixers	51
3.2.4	Sensor Housings.....	51
4	Initial Assembly	52
5	Sensor Calibration.....	53
5.1	pH Calibration	53
5.2	Flowmeter Calibration.....	55
5.3	Turbidity Calibration.....	56
5.3.1	Attempt One.....	57
5.3.2	Attempt Two	57
5.3.3	Calibration of dosing pumps.....	59
5.3.4	Jar Tests	61
6	Final Assembly and Tests	67
6.1	Final Assembly.....	67
6.2	Test Runs(Hopper Bottom)	68
6.2.1	Test Run One	68
6.2.2	Second Run (Hopper Bottom)	70
6.2.3	Test Run Three.....	71
6.2.4	One More Calibration	72
6.3	Final Operation Plan.....	75
6.3.1	Calibration.....	75
6.3.2	Operating Conditions	77
6.3.3	Precautions	78
6.4	Final Tests and Results	80
7	Conclusion	2
7.1	Modifications from original plan	2

7.2 Major issues encountered	3
References.....	4
Appendix A Arduino Code Programs.....	7
A1 Motor Control Code for the Water Pump.....	7
A2 Turbidity Sensor Calibration Code.....	7
A3 PH Sensor Calibration Code.....	8
A4 Dosing Pump Testing Code.....	9
A5 Flowmeter Testing Code	9

List of Figures

Figure 2-1 Diagram of Water Treatment Process (How Is Water Treated for Homes by Alyssa Hensler).....	7
Figure 2-2: The electric potential in relation to the distance from the surface of the particle.....	8
Figure 2-3: Mechanism of a Plate-Type Static Mixer (Westfall, Inline Static Mixer)	13
Figure 2-4: Mechanism of the Housed-Elements Mixer.....	13
Figure 2-5: (Process Engineering: Agitation and Mixing, by Prof. Mihir Shah, DDU) A basic design with an agitator with a lower radial impeller and an upper axial impeller inside a draft tube.....	16
Figure 2-6: Types of Impellers (Process Engineering: Agitation and Mixing, by Prof. Mihir Shah, DDU).....	18
Figure 2-7: Design Processes for blending and motion, solids suspension and gas dispersion (Liquid Agitation, by Lewis E. Gates& Terry L. Henley, 1985).	20
Figure 2-8: Log-log plot of power number as a function of Reynolds for Rushton, pitched blade and hydrofoil turbines (Thermopedia).....	21
Figure 2-9: Traditional (circular) Clarifier(Clarification—Boiler Technologies, ESC Energy Solutions Center).....	23
Figure 2-10: Flow patterns for lamella clarifiers (a) countercurrent (b) cocurrent (c) crosscurrent (Davis, 2010)	25
Figure 2-11: Hopper bottom settling tank (Leheng)	26
Figure 2-12 Example of an open-loop control system (Control System,TutorialsPoint).....	35
Figure 2-13 A closed-loop control system (Control System,TutorialsPoint).	35
Figure 2-14 Overview of the direct-filtration system (Michigan Technological University)	37
Figure 2-15 Application Steps in Laboratory Studies.....	39
Figure 3-1: P&ID diagram for the preparatory schematic of the system.	41
Figure 3-2: Motor control with a transistor.....	41
Figure 3-3: Schematic of an L298N Dual H-Bridge Motor Driver (Handson Technology)	42
Figure 3-4: Electronic Schematic of the TSD-10 Turbidity Sensor (Electro Schematics)	44
Figure 3-5: the Relationship between turbidity and voltage (Electro Schematics)	45
Figure 3-6 Zeta-Potential Cell.	47

Figure 3-7: Lab Conventional Clarifier	48
Figure 3-8: Lab Hopper-Bottom Clarifier.....	48
Figure 3-9: Lab Lamina Clarifier.....	49
Figure 3-10 Lab Filtration Column.....	50
Figure 3-11 Turbidity and pH Housing	51
Figure 4-1: P&ID diagram for one of each sensors (flowrate, turbidity and pH).....	52
Figure 5-1 relationship between voltage and pH for pH Sensor One	54
Figure 5-2 Linear Relation between Voltage and pH for pH Sensor Two	55
Figure 5-3 Turbidity Voltage Readings VS NTU.....	57
Figure 5-4 Voltage VS Turbidity for Turbidity Sensors' Calibration	59
Figure 5-5 Aluminium Sulphate Dose VS Turbidity.....	62
Figure 5-6 Second Test Result Plot	63
Figure 5-7 Third Jar Test Graph	64
Figure 5-8 Jar Test 4 Turbidity Plot.....	65
Figure 5-9 Jar Test 4 Plot Zeta Potential VS $Al_2(SO_4)_3$ Concentration	65
Figure 6-1 Final Assembly Schematic	67
Figure 6-2 Sample Water Container	68
Figure 6-3 Sample Water After 9 Minutes in Test Run One	69
Figure 6-4 Filtration Column Leaks	72
Figure 6-5 Turbidity VS Voltage.....	73
Figure 6-6 pH VS Voltage	74
Figure 6-7 pH VS Voltage	75
Figure 6-8 schematic of the assembly illustrating the height difference	79

List of Tables

Table 2-1 Maximum acceptable values for inorganic determinands of health significance(Drinking-Water Standards for New Zealand)	6
Table 2-2 most commonly used coagulants (American Water College, 2018)	9
Table 2-3 Common Coagulant Combinations (American Water College, 2018).....	10
Table 2-4: Average Zeta Potential corresponding to degree of coagulation (American Water College, 2018).....	11
Table 2-5 Polymer Flocculants and Their Contents	12
Table 5-1 Calibration Data of pH Sensor One.....	54
Table 5-2 Calibration Readings from pH Sensor 2.....	55
Table 5-3 Calibration Data of the Flowmeter	56
Table 5-4 Arduino Turbidity Readings for Calibration Attempt One	Error! Bookmark not defined.
Table 5-5 Calibration Data for Turbidity Sensors (Attempt Two)	59
Table 5-6 Calibration Data for Dosing Pumps	60
Table 5-7 Jar Test Result One.....	61
Table 5-8 Second Test Result	62
Table 5-9 Fourth Jar Test Result.....	64
Table 6-1 Flowrate and Turbidities measured for Run 2 of Hopper Bottom Clarifier.....	70
Table 6-2 Flowrate and Turbidities measured for Run 3 of Hopper Bottom Clarifier.....	71
Table 6-3 Turbidity VS Voltage.....	72
Table 6-4 pH VS Voltage	74
Table 6-5 pH VS Volage.....	74
Table 6-6 Results of Run One	Error! Bookmark not defined.
Table 6-7 Results of Run Two.....	1
Table 6-8 Results of Run Three	2
Table 6-9 Results of Run four.....	2
Table 6-10 Results of Run Five	2
Table 6-11 Results of Run Six	3
Table 6-12 Results of Run Seven.....	3
Table 6-13 Results of Run Eight.....	3

Table 6-14 Results of Run Nine.....4

1 Introduction

1.1 Overview

Access to fresh water is one of the largest drivers to building a modern society.

Clean water in urban settlements generally comes from natural water bodies such as lakes and rivers, where water contains impure matter like bacteria, tree branches, grains of stone, as well as some chemicals that need to be removed. A water treatment process to purify the water of the aforementioned substances is therefore necessary (Kerry J. Howe ,2012).

Water purification process, generally speaking, involves coagulation-flocculation, sedimentation, filtration and disinfection.

Coagulation-flocculation is the process of adding chemicals, such as aluminium sulphate or ferric chloride, that neutralize the charge of small particles in the water and then aggregate them into bigger clusters (floc).

Sedimentation is the process of settling down floc produced in the coagulation-flocculation process, along with other particles in suspension. This is usually achieved by slowing down of the water flow for the particles in suspension to gradually settle down before moving on to the next stage. The sediment that settled down at the bottom of the sedimentation tank (clarifier) is regularly removed at a certain time interval. An alternative to sedimentation is to aerate the water to float the floc and other sizeable particles to the top surface of the water with a sweeping arm to skim away the scum regularly.

Filtration is the separation of solid matter from water with usually layers of filters which enable the water to pass through but not the solid matter.

In most cases a final treatment of disinfection is also included to remove the remaining chemicals and bacteria previous stages did not remove. The most common method is adding chlorine into the water to kill any bacteria still remaining. An alternative disinfection method is using ultra-violet radiation to kill of the bacteria.

The goal of this project is to build three separate microscopic water treatment systems, each with a different sedimentation tank (clarifier), a conventional, a hopper bottom and a laminar clarifier. Further details will be covered in later chapters of the thesis.

1.2 Problem Statement

The environmental lab of the University of Waikato has three settling tanks, a hopper-bottom tank, a laminar tank and a conventional tank.

The tanks need to be installed into a water treatment system, with flocculant dosing before, and a filtration column after, to form a water treatment system so that undergraduate student can study the water treatment process at a lab scale.

The system also needs to be fitted with Arduino sensors to read pH values, turbidity values and the flowrate which are controlled by an Arduino coding to give student data for the treatment process and to automatically control the dosing and flowrate.

1.3 Project Aims

The project aims to install, for the engineering lab, three separate microscopic water treatment systems, all consisting of the flocculation & coagulation, the sedimentation and the filtration phases, each with a different type of clarifier (sedimentation tank)--- a conventional clarifier, a laminar clarifier and a hopper bottom clarifier.

All three systems are to be connected with instruments measuring pH, zeta potential, the flow rate, turbidity, and particle size.

The instruments need to be coupled to an Arduino to control the coagulation & flocculation based on the flow rate, turbidity and zeta potential.

The instrumentation should also be able to log measured data for students to collect and analyse.

1.4 Structure of the Thesis

A general literature review is covered in Chapter 2. This includes the theory of dosing (coagulants and flocculants), mixing, and the general principles and theory about the clarification as well as filtration, followed by summaries of two theories related to this project, including several measurement theories, control theories. And after that, two

brief summaries of two research theses, one on installation of a lab filtration column and the other on the study of Arduino for university teaching.

Chapter 3 is an introduction of components used, both electronic and physical. Electronic components include two turbidity sensors, two pH sensors and a self-assembled zeta potential meter. 3D printed housings were made to fit in the turbidity sensor and the pH sensor. Water tanks for settling, mentioned at the beginning of the thesis, are provided by the lab. Two static mixers, one rapid and one slow, were 3D-printed for mixing of the sample with the flocculant. The filtration column is provided by the lab.

The fourth chapter is a brief summary on a simple test assembly to ensure the coordination of the Arduino code, the electronic components were working properly and the pump was tested for its functionality as well.

Chapter 5 documents the calibration results. The flowrate sensor was calibrated once and has been accurate without problems. But the turbidity and pH sensors, due to their fluctuation, need to be recalibrated frequently to restore their accuracy. The zeta potential meter was calibrated too, with only a voltage reading, no mathematical conversion is needed. The turbidity and pH values fluctuated significantly out of each calibration, indicating that recalibration is needed constantly, preferably right before the experiments to minimise error. As a result, these calibration results do not conclude the calibration of turbidity and pH sensors, further calibration required right before the experiments.

Chapter 6 addresses the process of the running of the system itself, starting with the final assembly schematic, several pre-runs to ensure the smooth functioning of the system, a final operation plan elaborating mathematical and procedural details of the experiments, precautions on potential glitches, and concluded by result data collected from the series of experiments.

The final chapter, Chapter 7, gives conclusions and discussions of the whole research project, detailing problems encountered and compromises made, with suggestions to improve the process in the future.

2 Literature Review

2.1 Overview

According to the online article *Methods of Water Purification Ancient to Modern* (April 3rd, 2020) The treatment of potable water can be traced back to ancient civilizations. As early as 4000 B.C. the Sanskrit text, *Sushruta* recommended that water should be boiled or heated and filtered with charcoal and gravel before consumption by humans.

However, significant breakthroughs in the water treatment technology did not occur until the 19th century, when Britain, the United States and other continental European countries started implementing municipal filtration systems in densely populated cities as water pollution became an increasingly serious issue due to industrialization and the increased sewage discharged into rivers like the Thames. Diseases like cholera also caused stricter measure implemented in municipal water treatment.

By the late 19th century, chlorination started to be used as a disinfectant in water treatment systems to kill bacteria. This became increasingly popular in the early 20th century.

Contaminants in water include large pieces of debris, like tree branches, rocks, solutes, colloids, solid suspended matter and bacteria. Different treatment processes are required to remove each of these impurities. In general primary screening is to remove sizable contaminants. Certain chemicals are applied to remove undesirable chemicals as well as bacteria, which is killed by chlorination. Coagulation and flocculation are applied to remove other impurities such as colloids, and suspended particles.

Water treatment in New Zealand needs to comply with the *Drinking-Water Standards for New Zealand*, a piece of legislation first passed in 2005 and last revised in 2018. The Standards include mainly two themes, the maximum acceptable values and the compliance criteria. Table 2-1 shows the acceptable values for inorganic substances in the *New Zealand Drinking-Water Standards*. More information, including acceptable values of organic matter, more information, including organic standards, microbial standards and aesthetic standards, can be found in *Drinking Water Standards for New Zealand* itself on Pages 7 to 12.

Table 2-1 Maximum acceptable values for inorganic determinands of health significance

Name	MAV(mg/L)	Remarks
antimony	0.02	
arsenic	0.01	For excess lifetime skin cancer risk of 6×10^{-4} . PMAV, because of analytical difficulties
barium	0.7	
boron	1.4	
bromate	0.01	For excess lifetime cancer risk of 7×10^{-5} . PMAV
cadmium	0.004	
chlorate	0.8	PMAV. Disinfection must never be compromised. DBP(disinfection by-product) (chlorine dioxide)
chlorine	5	Free available chlorine expressed in mg/L as Cl ₂ . ATO. Disinfection must never be compromised
chlorite	0.8	Expressed in mg/L as ClO ₂ . PMAV. Disinfection must never be compromised. DBP (chlorine dioxide)
chromium	0.05	PMAV. Total. Limited information on health effects
copper	2	ATO
cyanide	0.6	Total cyanides, short-term only
cyanogen chloride	0.4	Expressed in mg/L as CN total. DBP (chloramination)
fluoride	1.5	
lead	0.01	
manganese	0.4	ATO
mercury	0.007	inorganic mercury
molybdenum	0.07	
monochloramine	3	DBP(chlorination)
nickel	0.08	
nitrate, short-term	50	Expressed in mg/L as NO ₃ . The sum of the ratio of the concentrations of nitrate and nitrite to each of their respective MAVs must not exceed one
nitrite, long-term	0.2	Expressed in mg/L as NO ₂ . PMAV (long term)
nitrite, short-term	3	Expressed in mg/L as NO ₂ . The sum of the ratio of the concentrations of nitrate and nitrite to each of their respective MAVs must not exceed one
selenium	0.01	
uranium	0.02	PMAV

Abbreviations:

- (1) DBP: disinfection by-product.
- (2) ATO: Concentrations of the substance at or below the health-based guideline value that may affect the water's appearance, taste or odour.

The processes, in most conventional water treatment plants, consist of primary screening, coagulation and flocculation, sedimentation, filtration and disinfection, as shown in the figure below.

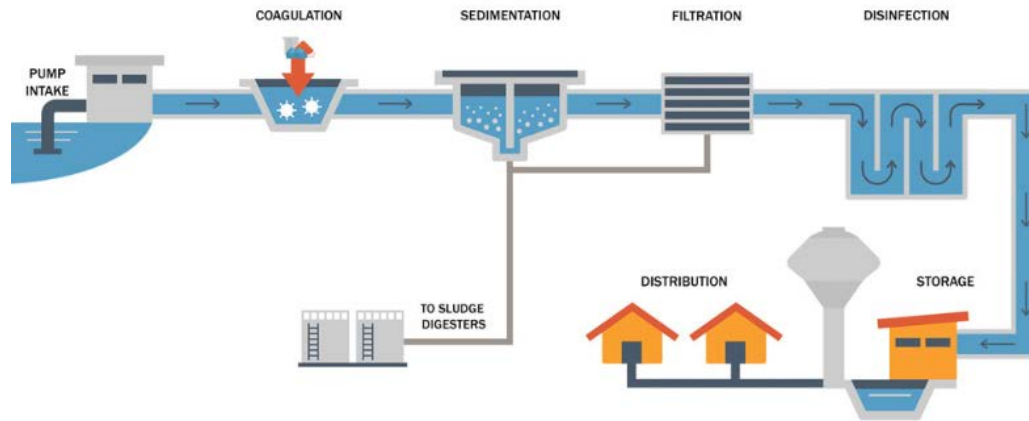


Figure 2-1 Diagram of Water Treatment Process Primary Screening(Hensler, 2018)

Primary Screening is a simple physical process, usually at the beginning of the treatment system, to screen out sizable chunks of debris like wood, rocks, large water plants .etc. Screens of various dimensions of gaps are placed before water enters the water treatment plant. Debris of different sizes gets caught by these screens, making the initial step of purification before water gets pumped to the plant for the next treatment step (Ambulkar,2018).

2.2 Coagulation and Flocculation

Coagulation and flocculation are steps to eliminate certain mainly colloids, and along with some solutes, that are stabilised in the water treated so they either do not settle or take too long to settle without coagulation and flocculation (Bratby, 2016)..

Colloids in water mostly have a negatively charged surface. The charge is proportional to the total surface area. Hence, for a given mass of colloids, the more divided they are, the greater the ratio of total surface area to mass, the more charge they carry in total (Bratby, 2016). When the colloids get closer, the negative charges repel each other, preventing them from agglomerating into big-enough clusters to be removed by settlement or filtration. The electric potential formed by the electric charge on the surface between the colloid and the medium is called the zeta potential (McNaught & Wilkinson, 1997).

With colloids, the term stability is used to describe the ability of individual colloids to remain dispersed in the suspension. The two major factors that determine the stability of a suspension are (i) the surface charge at the interface between the colloid and the

medium (water in this case) and (ii) the hydration of surface layers of the colloid (Bratby, 2016).

The double layer structure often forms on solid particles in water. The first layer consists of ions adsorbed onto the surface of the particle as a result of chemical reactions and is relatively immobile. The second layer are ions oppositely charged to the first layer and adhering to the first layer through the Coulomb force. The stern model is one of the models to study the double layer structure, with the first layer (inner layer) being the stern layer comprising ions oppositely charged to the surface of the particle. The Stern potential is the difference between the out boundary of the stern layer and the bulk solution (Bratby, 2016). Figure 2-1 gives a diagrammatic description of the stern potential.

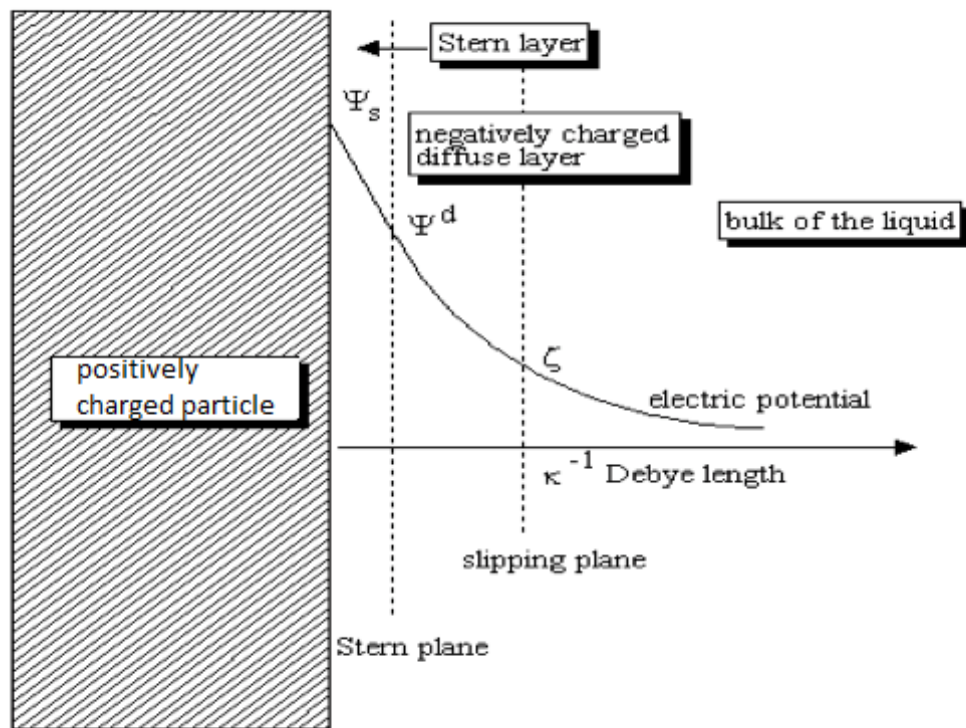


Figure 2-2: The electric potential in relation to the distance from the surface of the particle (Bratby, 2016).

Coagulants are chemicals added into the aqueous suspension to neutralize the surface charges of the colloids so it becomes easier for them to collide and cluster together by Van der Waals forces (Bratby, 2016). The term primary coagulant is often used to refer

to the chemicals acting as the neutralization agent for the coagulation-flocculation process as opposed to other chemicals to aid the same process such as flocculation aides.

The most commonly used primary coagulants are aluminium based or iron based compounds. Alum (aluminium sulphate) is currently the most widely used coagulant in municipal water coagulation among metallic coagulants. Iron based coagulants include ferrous sulphate, ferric chloride, ferric sulphate and ferric chloride (Bratby, 2016). Other coagulants include hydrated lime and magnesium carbonate (Bratby, 2016).

In general, trivalent coagulants (carrying 3 positive charges) are more effective than bivalent coagulants (carrying 2 positive charges) and monovalent coagulants (carrying 1 positive charge) given that it carries more charges for the same amount of dosage (Coagulation Chemistry Basics, July 2020).

The choice of what coagulant to use also depends on the pH of the water, the efficiency of rapid mixing and the dosage required of the coagulant (Bratby, 2016).

Table 2-1 shows a list of commonly used coagulants.

Table 2-2 most commonly used coagulants (American Water College, July 2020)

Chemical	Formula	Remarks
Aluminium Sulfate	$Al_2(SO_4)_3 \cdot 14(H_2O)$	Most common-often used with cationic polymer
Aluminium Chlorohydrate	$Al_2Cl(OH)_5$	Produces less sludge and corrosivity
Ferric Chloride	$FeCl_3$	Effective over wider pH range than alum
Ferric Sulphate	$Fe_2(SO_4)_3$	Often used with lime softening
Ferrous Sulphate	$Fe_2(SO_4)_3 \cdot 7(H_2O)$	Less pH dependent than alum
Aluminium polymers	–	Polyaluminium chloride(PAC)- Polyaluminium sulphate
Cationic polymers	–	Large molecule, synthetic polyelectrolytes
Sodium aluminate	$Na_2Al_2O_4$	Improves alum coagulation
Sodium silicate	$Na_2 \cdot (SiO_2)_x$	Used to make coagulant aid activated silica(x=0.5-4.0)

It is also widely practiced to combine more than one coagulant to form mixed coagulants. Table 2-1 gives a list of common combinations of coagulants to enhance the coagulation process. Combining alum with caustic soda or lime for example, helps optimize the pH of the treated water (Gebbie, 2006).

Table 2-3 Common Coagulant Combinations (American Water College, 2018)

Coagulant Combinations	Ratio
Aluminium sulphate + caustic soda	3:1
Aluminium sulphate + hydrated lime	3:1
Aluminium sulphate + sodium aluminate	4:3
Aluminium sulphate + sodium carbonate	1:1 to 2:1
Ferric sulphate + hydrated lime	5:2
Ferrous sulphate + hydrated lime	4:1
Ferrous sulphate + chlorine	8:1
Sodium aluminate + ferric chloride	1:1

The dosage of the primary coagulant should ideally be just enough to neutralise all zeta potential without overdosing which introduces the primary coagulant as the new impurity that needs to be removed. In reality, though, it is impractical to reach the perfect amount of coagulant without under- or overdosing to a degree (Bratby, 2016).

The amount of coagulant added into the water treated should be controlled within a certain range to avoid incomplete neutralization or excessive coagulant becoming the new impurity.

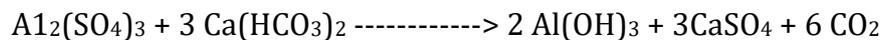
Table 2-3 gives a list of ranges of zeta potential corresponding to their degrees of coagulation.

Table 2-4: Average Zeta Potential corresponding to degree of coagulation (American Water College, 2018)

Average Zeta Potential (V)	Degree of Coagulation
0 to +3	maximum
-4 to -1	excellent
-10 to -5	fair
-20 to -11	poor

As the table shows, the maximum zeta potential range is 0 to +3, more than which the coagulant would be excessive and causing new impurity. -4 to -1 is an excellent range. -10 to -5 is still acceptable.

As already stated, alum is currently the most widely used coagulant (Bratby, 2016). The chemical reaction of coagulation by alum is as follows:



After coagulation, the Van Der Waals forces pull together the no longer charged colloids together to form small flocs. Flocculation, the process ensuing the coagulation process, is to further agglomerate the small flocs together into bigger flocs to make it easier to be eliminated by sedimentation or filtration (Bratby, 2016).

Flocculation, in general, consists of perikinetic flocculation and orthokinetic flocculation. Perikinetic flocculation refers to the clustering of colloids due to the random motion of colloids. Orthokinetic flocculation refers to flocculation as a result of the bulk motion of the fluid, such as stirring (Bratby, 2016).

The flocculation process is achieved by different stages of mixing. At each stage, the water is agitated to increase collision between flocs, which cause them to agglomerate. The mixing energy, which depends on the agitation, generally decreases throughout the stages, given that the flocs increase in size after each stage, needing less and less collision (Bratby, 2016).

Certain types of polymer are often used as a flocculation aid to enhance the flocculation process. The table below presents several types of common polymeric flocculants and their most common content:

Table 2-5 Polymer Flocculants and Their Contents (Bratby, 2016)

Polyacrylamides	5-10%
Polyamines	20-50%
PolyDADMs	10-98%
Resin Amines	6-10%

The performance of flocculation is generally governed by two factors, the velocity gradient and the time of mixing. The velocity gradient is the difference in velocity between layers of the fluid flowing through a pipework, with respect to proximity to the sides of the pipe. This causes particles to come into contact and agglomerate. And the longer the mixing time, the more time the particles have to agglomerate (Bratby, 2016).

2.3 Static Mixers

Static mixers are also known as inline mixers. They are fitted in line with the tubing of the fluid. The two most common types of static mixers are plate-type mixers and housed-elements mixers. Both types achieve mixing by interrupting the smooth flow of the liquid, causing turbulence, thus increasing the mixing energy (REF).

A plate-type static mixer has plates added inside the pipe to interrupt the smooth flow of the liquid, causing it turbulence and increasing the mixing of between the liquid and the chemical added, as Figure 2-2 demonstrates.

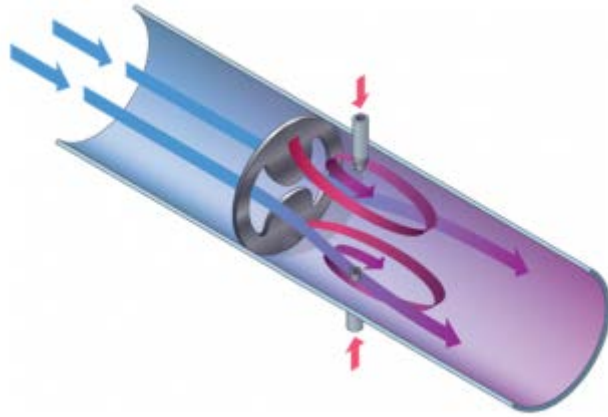


Figure 2-3: Mechanism of a Plate-Type Static Mixer

A more common type is the housed-elements type, in which the inside of the housing of the mixer is fitted with a series of baffles, typically in helical shape, that when the fluid flows through them, they cause turbulence of the fluid to facilitate it blending with the added chemical, as demonstrated in Figure 2-3 (Koflo, July, 2020).



Figure 2-4: Mechanism of the Housed-Elements Mixer (Koflo, July, 2020)

The performance of static mixing depends on several parameters, including the diameter of the housing (the Reynolds number is proportional to the diameter) or properties of the fluid itself (viscosity, for example, to which the Reynolds number is inversely proportional), the number of baffles and their design (Koflo, July, 2020).

As shown in Figure 2-3, helical baffles in a static mixer can simultaneously generate flow division and radial mixing (Koflo, July, 2020).

With flow division, each edge of the baffle element causes the fluid to split into two laminar streams, which is repeated every time the fluid flows through another edge, leading to the increase of stratification. The number of striations (the number of split streams) equals 2^n where n is the number of elements inside the mixer. The quality of the mixture is therefore a function of the mixer diameter and the number of elements, independent from the flowrate and viscosity of the fluid (Statiflo, July, 2020).

Radial mixing is caused by rotational spin generated by the shape of the elements. The fluid is constantly spun away from the centre of the pipe towards the wall and then back, rapidly blending together the fluid and added chemical by eliminating radial differences in colour, composition, pH, temperature and viscosity. Radial mixing requires fewer elements to achieve mixing than flow division (Bratby, 2016).

One disadvantage of static mixers is that with caustic chemicals added, they can build up corrosion on the elements, causing the flow being clogged (Bratby, 2016).

The coefficient of variation defined as the ratio of the standard deviation to the mean, is often used in the mixing theory. Compared with the standard deviation, the coefficient of variation takes factors in the numerical sizes of each sample rather than only the absolute amount of deviation. The equation is as follows:

$$C_v = \frac{\sigma}{\mu}$$

Where c_v is the coefficient of variation, σ the standard deviation and μ the population mean. The lower the c_v , the better the mixing quality (Bratby, 2016).

2.4 Tank Mixing

Tank mixing consists mainly of passive mixing and active mixing. This section gives details on the variation of mixing techniques used on each of them.

2.4.1 Passive Systems

A passive mixing system is a system where the mixing process does not require extra power. This does not mean a passive system uses no external power, but that the external power used (for the pump etc.) is limited to providing locomotion rather than the mixing process itself (Duer, 2011).

The mixing efficiency of passive mixing systems depends on various factors including the velocity difference between the inlet jet and tank water, the temperature, the positions of the inlet and outlet separation and the number of inlet ports (Duer, 2011).

Difference of velocity between the inlet jet and the tank water generates turbulence, which then generates circulation patterns which mixes the original tank water and the newly added inlet water. All shapes of tanks develop circulation patterns, although the pattern itself depends on the geometry of the specific tank itself (Duer, 2011).

Complete mixing is achieved if a fill cycle lasts longer than the minimum time needed for complete mixing, represented by the following equation (Duer, 2011):

$$\tau_m = K' \frac{V^{2/3}}{M^{1/2}}$$

Where τ_m is the mixing time,

K' is an experimental constant (≈ 10.2) for a single inlet with no temperature difference between inlet and tank water,

V is the volume of the tank,

M is the inflow momentum, the product of the velocity and the flow rate.

Separating the inlet and outlet pipes is becoming more common in water treatment nowadays. Counterintuitive as it seems, though, the optimal location is not when maximizing the distance between the inlet and outlet pipes. The optimal location of the outlet depends on the circulation pattern of the tank, which in turn is determined by the tank style and the inlet (Duer, 2011). With a proper design, however, the location of the outlet should not be crucial to the mixing efficiency if the with enough mixing time for a thorough mixing of the water.

The temperature difference between the inlet and tank water can cause problems for the mixing, especially during summer, when the tank water tends to be significantly warmer than the inlet water. Since the density of water decreases with temperature, the inlet water tends to sink towards the bottom of the tank, leaving the top water over-aged without mixing. (Duer, 2011).

2.4.2 Agitators

Agitation is often used to enhance the process of mixing. An agitator consists of a shaft, attached to a motor, and an impeller. When the motor is turned on, the rotary motion of the agitator causes the rotary motion of the liquid, thus enhancing the mixing process. Figure 2-4 shows a basic design of a mixing tank with an agitator installed (Bratby, 2016).

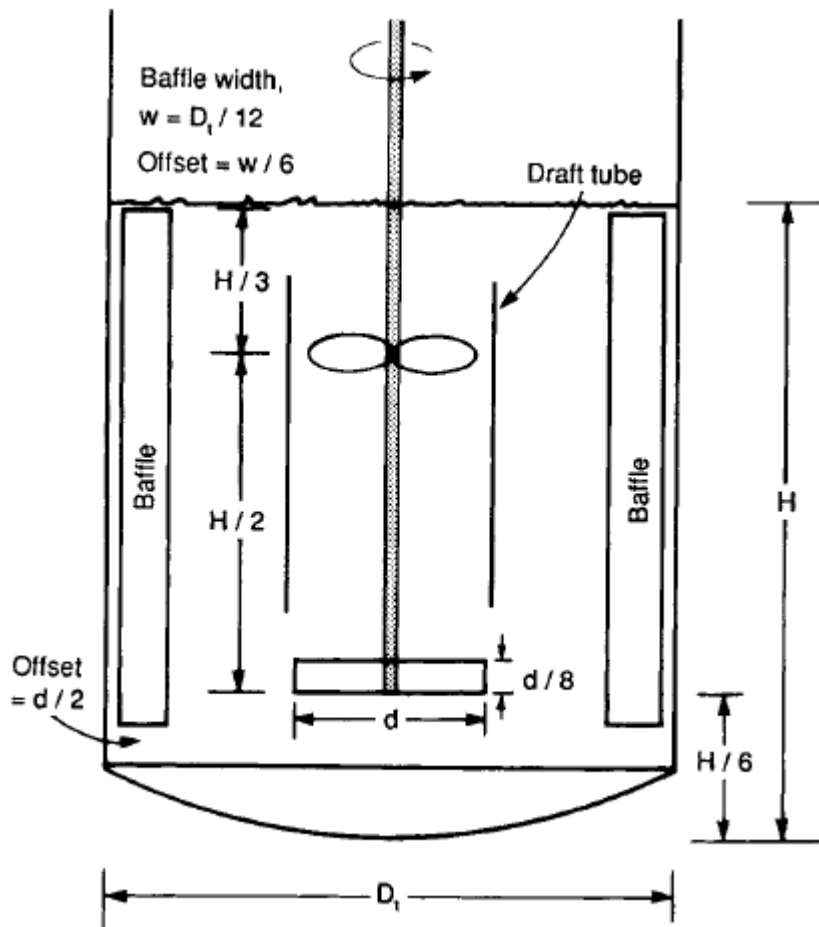


Figure 2-5: A basic design with an agitator with a lower radial impeller and an upper axial impeller inside a draft tube(Shah, DDU, July 2020).

As is shown in Figure 2-4, the agitation tank has baffles and a draft tube installed together with the tank and agitator.

Except at very high Reynolds numbers, baffles are needed to provide stability of the liquid by preventing vortexing and rotation of the whole liquid mass. The width of the baffles is usually $w=D_t/12$, a twelfth of the diameter of the tank. By standard, there are usually four baffles equally spaced around the inner wall of the tank (Bratby, 2016).

A draft tube is a cylindrical housing around the agitator. Ideally it should be barely wider than the diameter of the impeller. The draft impeller is used to direct suction and discharge streams along with the axial impeller, shaping a certain mixing flow pattern that would not result from the system itself (Bratby, 2016).

Several classifications of impellers exist. The most common classification is based on whether the motion is axial or radial, as Figure 2-4 shows. An axial impeller generates motion that is parallel to the axis of the shaft of the agitator while a radial impeller generates motion that is perpendicular to the shaft (Bratby, 2016).

Different shapes of impellers are used in the mixing process. Figure 2-5 shows some of the most common shapes of impellers used for agitation in the mixing process. Impellers are generally divided into three categories---- turbine impellers, paddled impellers and blade impellers. For blending and motion, turbine impellers are commonly used (Bratby, 2016).

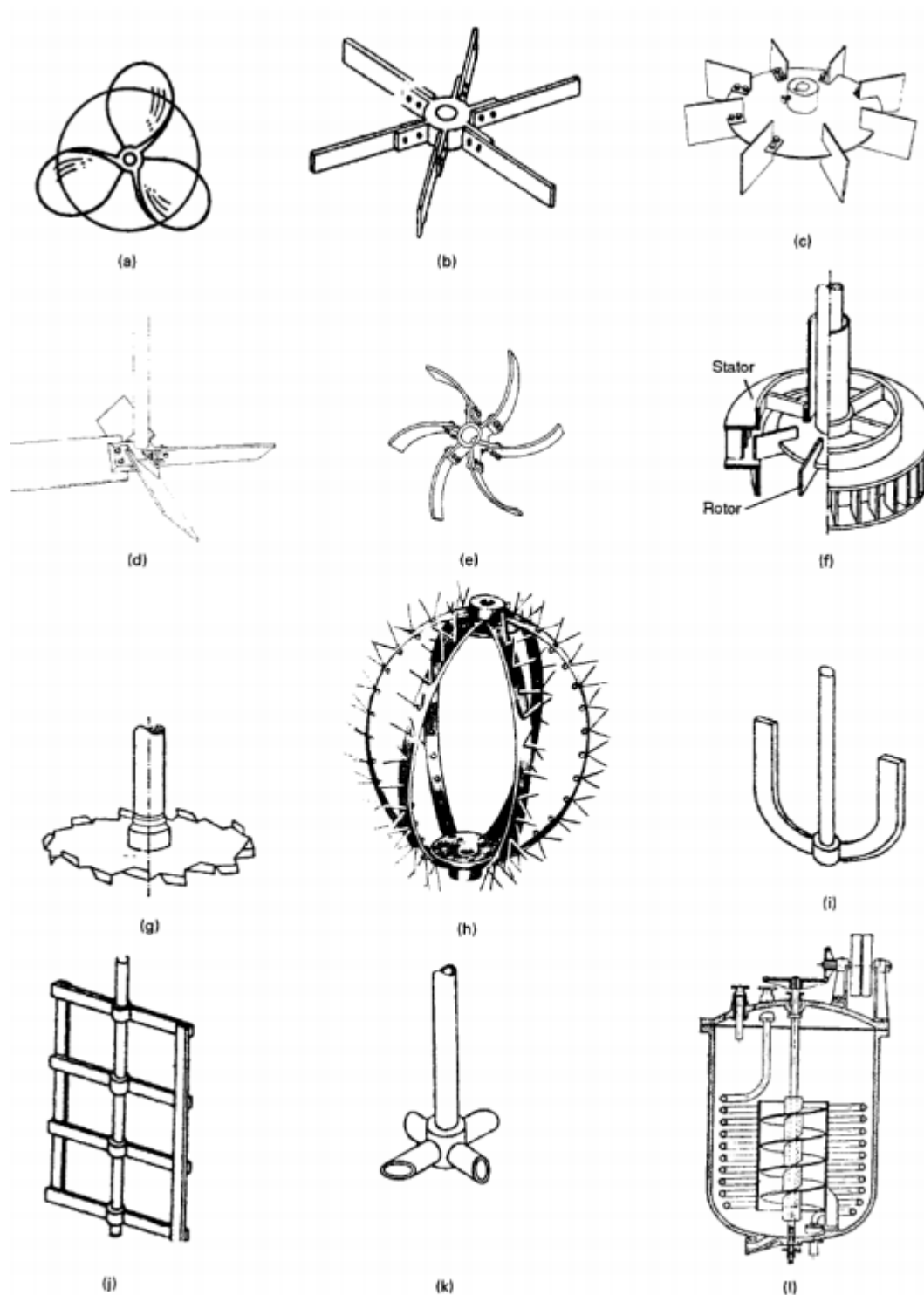


Figure 2-6: Types of Impellers (Shah, July, 2020)

The design of agitators, unlike most areas in engineering, lacks quantifiable standards that enable design engineers to work through the design process mathematically.

Reasons for this include the wide range of the application of agitators in process engineering, the absence of uniformly agreed-upon criteria to measure the performance of agitation, and the relatively complex nature of the application of agitators in the process engineering industry (Lesis & Terry, 1985, p.3).

Consequently, the written specification of agitators is often imprecise, giving different statements on the requirement of the degree of agitation, such as adequacy to promote reaction, maximizing contact between two phases(solid & liquid e.g.), blending two fluids to uniformity, or maximizing the dispersion of gas (Lesis & Terry, 1985).

Though not standardised officially, a classification of the agitator design process into three categories has been established. The three categories are based on the phases of the substances involved in the agitation, whether they are solids, liquids or gases. The design focus differs accordingly depending on the category of phases the agitator is meant to work with. Figure 2-6 shows three different design processes based on the phases involved in the process (Lesis & Terry, 1985).

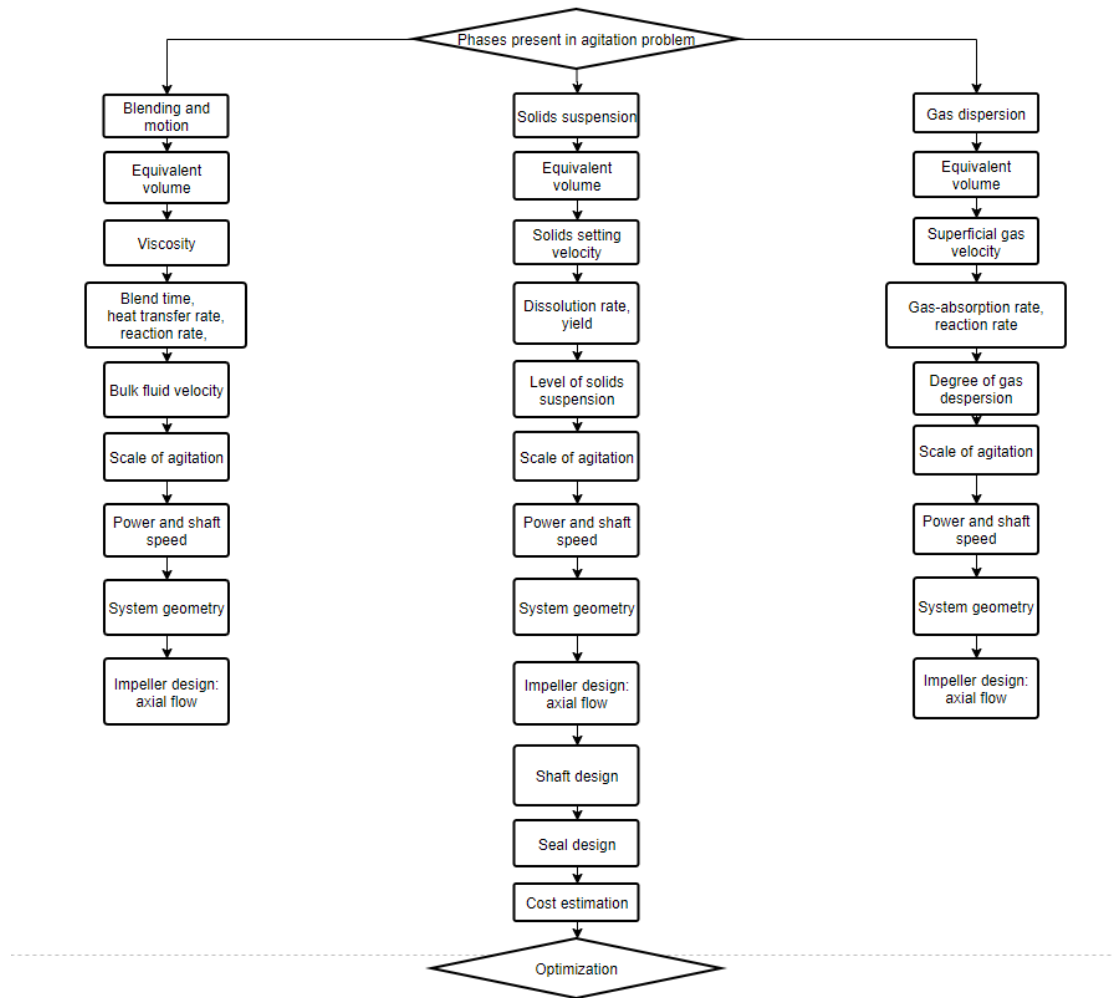


Figure 2-7: Design Processes for blending and motion, solids suspension and gas dispersion (Henley, 1985).

The magnitude of the agitation problem depends on how much material there is to agitate, how difficult the agitation is and the degree of agitation required (Henley, 1985).

An equivalent volume is often used to calculate the size and difficulty of the agitation. The equivalent volume is defined by the following equation (Henley, 1985):

$$V_{eq} = S_q V$$

Where S_q is the specific gravity and V is the actual volume.

Primary variables are variables used to define the degree of difficulty of agitation. The primary variable is viscosity in the case of blending and motion (Henley, 1985).

A dynamic response is a term used to specify the degree of agitation. In liquid-liquid mixing or reaction, the dynamic response is the bulk fluid velocity (Henley, 1985).

Given the dynamic response, the selection of equipment that meets the process requirements is then conducted. Pieces of equipment concerned are the primary move (the motor), the impeller system, and shafts and seals (Henley, 1985).

An economic evaluation of the equipment is part of the consideration along with the functionality concerns.

Design of agitators needs to calculate the power needed for the prime move. This is done by the power number versus Reynolds number graph. Figure 2-7 is a graph with power number versus Reynolds number of four types of turbines (Henley, 1985).

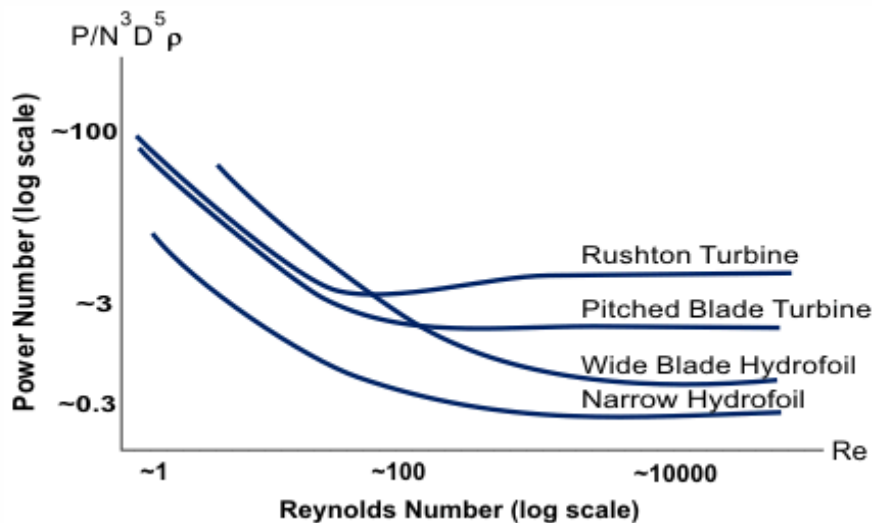


Figure 2-8: Log-log plot of power number as a function of Reynolds for Rushton, pitched blade and hydrofoil turbines (Thermopedia, July,2020).

The Reynolds number is a number describing a fluid’s state of chaos. It is calculated by the following equation:

$$Re = \frac{\rho u D}{\mu}$$

Where:

Re is the Reynolds number,

ρ is the fluid density(kg/m³),

u is the flow speed(m/s),

D is the diameter of the tube (m),

μ is the dynamic viscosity of the fluid(Pa · s).

And the power number is defined by the equation:

$$N_P = \frac{P}{\rho n^3 D^5}$$

Where

N_P is the power number,

P is the power,

ρ is the fluid density,

N is the rotational speed,

D is the diameter of the stirrer.

2.5 Settling Tanks

After coagulation and flocculation, the water needs to go through a sedimentation tank (clarifier) for flocs, colloids and other particles to settle to the bottom to be removed from the water.

The sludge formed by the settled particles at the bottom of the clarifier is removed either by a conveyer belt, a vacuuming pipe (especially in a hopper bottom clarifier), or a scraper (Bratby, 2016).

Clarifiers used for water treatment include the conventional clarifier, the hopper-bottom clarifier and the laminar clarifier (Bratby, 2016).

2.5.1 Conventional Clarifier

A conventional clarifier is a rectangular or circular pond with a certain surface area to slow down the flow of the treated water (Bratby, 2016). Figure 2-8 shows the mechanism of a circular conventional clarifier.

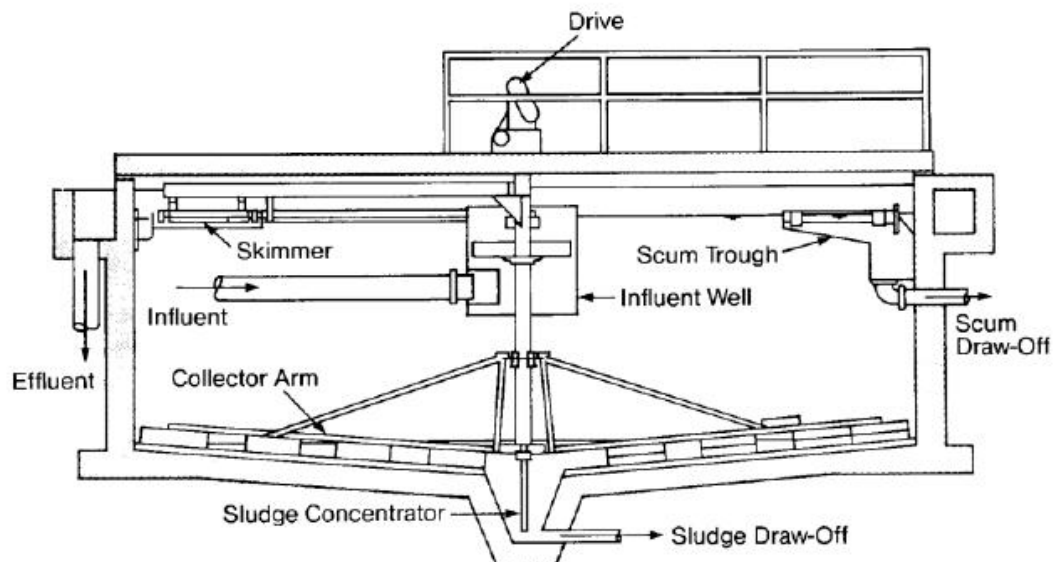


Figure 2-9: Traditional (circular) Clarifier (Clarification—Boiler Technologies, ESC Energy Solutions Center, July, 2020).

As the figure shows, the water enters the center of the clarifier and slowly moves radially towards the effluent at the circumference. As the flow of the water slows the suspended particles sink to the bottom of the tank, which then is swept into the sludge discharge by a collector arm at the bottom of the clarifier. It is also worth noticing that at the surface of the water there is a skimmer. This works in a similar way as the collector arm at the bottom, rotating to skim away the scum that floated to the top of the water (Clarification—Boiler Technologies, ESC Energy Solutions Center, July, 2020).

An important design parameter for sedimentation tanks is the surface loading rate defined as the maximum flow per day divided by the surface area of the tank, as expressed by the following equation (Clarification—Boiler Technologies, ESC Energy Solutions Center, July, 2020):

$$R_l = \frac{F}{A}$$

Where R_l is the surface loading rate (m/day), F the maximum daily flow (m^3/day) and A the surface area of the tank (m^2).

2.5.2 Lamina Clarifier

A lamina clarifier is also known as a lamella clarifier or inclined plate settler (IPS). It is a water tank with inclined plates in parallel which the suspended particles drop onto and slide down to the bottom of the tank to be removed out of the sludge discharge (Figure 2-9) (Davis, 2010).

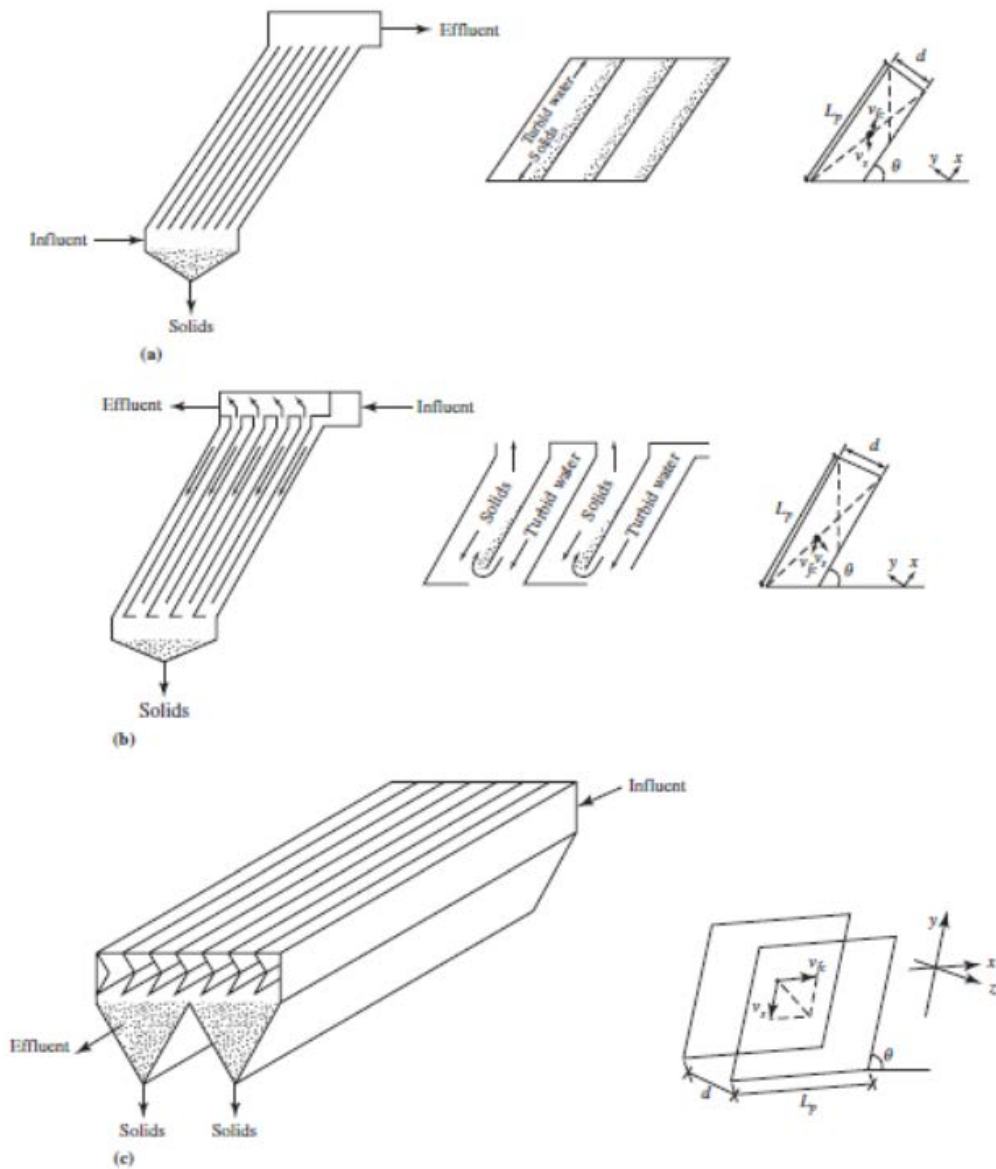


Figure 2-10: Flow patterns for lamella clarifiers (a) countercurrent (b) cocurrent (c) crosscurrent (Davis, 2010)

As Figure 2-9 shows, there are, in general, three types of lamella clarifiers---the countercurrent clarifier, whose water and sludge flows have opposite directions, the concurrent clarifier, whose water and sludge flow in the same direction and the cross current clarifier, whose water flow is perpendicular to the sludge flow (Davis, 2010).

According to Lytra (2019), concurrent clarifiers are more suitable when the sludge volume is a small percentage of the feed. In most circumstances, however, the countercurrent clarifier is more desirable than the other two types.

The total surface area of a lamina clarifier can be calculated with the following equation (Davis, 2010):

$$A = W \cdot (Np + \cos \theta)$$

Where A is the total surface area(m²), W is the width of the plates(m), N the number of plates, p the tube spacing(m), and θ the pitch angle(rads).

2.5.3 Hopper Bottom Clarifier

In a hopper bottom clarifier, the sludge accumulates at the hopper-shaped bottom of the sedimentation tank and is regularly removed through a discharge pipe (REF). Figure 2-10 shows the workings of a hopper-bottom clarifier.

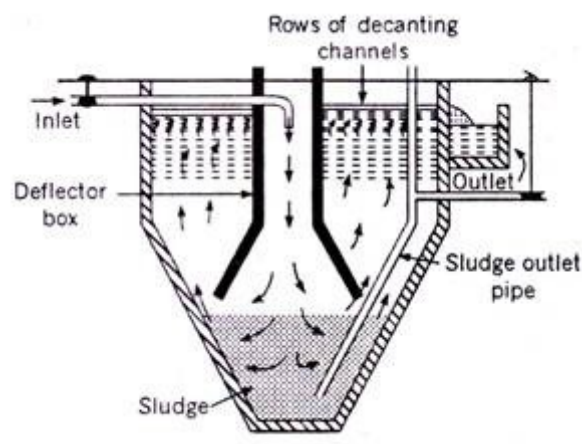


Figure 2-11: Hopper bottom settling tank (Types of Sedimentation Tanks, July, 2020)

As is shown in Figure 2-10, the water moves from the bottom towards the top of the tank as the cross-section widens upward. With a constant flow rate, the widening area causes the velocity of the water to decrease, facilitating the settling of particles in the water. The particles drop to the bottom of the tank and are removed by a sludge outlet pipe (Types of Sedimentation Tanks, July, 2020).

2.5.4 Settling Theory

The theoretical study of sedimentation has seen the contribution of Bernoulli (1700-1782), Euler (1707-1783), Saint-Venant (1797 - 1886), Darcy (1803-1858), Froude (1810-1879), Stokes (1819-1903), Reynolds (1842-1912) etc. Here we will focus mainly on the Saint-Venant Equation and the Stokes' Law.

The Saint-Venant equation is a specific form of shallow water equation when it is in unidirectional form. The Saint-Venant equation can be used to work out the water elevation needed for a rectangular tank. It can also describe the fluid motion when written in the following form (Degremont, 1991):

$$\frac{\partial u}{\partial t} + u \frac{\partial u}{\partial x} + w \frac{\partial u}{\partial z} = -\frac{1}{\rho} \frac{\partial p}{\partial x} + \nu \left(\frac{\partial^2 u}{\partial x^2} + \frac{\partial^2 u}{\partial z^2} \right) + f_x$$

Where x represents the horizontal coordinate, z the vertical; t is the time; u and w are the longitudinal and vertical flow velocities; p is the pressure of the flow; ρ is the density of the fluid; ν is the kinematic viscosity and f_x is the body force in the x direction (Wen Sun 2014).

The equation is the result of combining the continuity equation with the momentum equation, solving both of which together is rather difficult. Numerical techniques have been put forward to handle specific cases of the Saint-Venant equation. For example Mahmood and Yevjevich (1975) have provided methods to solve open-channel problems.

The Stokes' law states that the settling velocity of a particle is proportional to the particle's radius squared, by the following equation:

$$\omega = \frac{2}{9} \frac{g}{\mu} (\rho_p - \rho) R^2$$

where ω is the settling velocity of the particle (rad/s), g is the gravitational acceleration (m/s^2), ρ_p is the particle's density (kg/m^3), ρ is the fluid density and R is the radius of the particle (m) (Degremont, 1991).

Stokes' law is based on the assumptions that the flow is laminar, the particle is spherical, the surface is smooth, the material is homogeneous and that the particles are far away enough to not interact with each other at all (Degremont, 1991).

From the equation it is obvious that the settling velocity is mainly determined by the density difference between the fluid and the particle, and the radius of the particle.

Sizing of the settling tanks was governed by equations and principles given below from *the Basic Water Treatment* (Chris Binnie et al. July, 2020).

For horizontal clarifiers like a conventional clarifier, the size of the clarifier needs to guarantee the particles reach the bottom before reaching the outlet, governed by the following equation:

$$v_s/v = D/L$$

where v_s is the settling velocity (m/s) of the particle, v is the flowing velocity (m/s) of water, D is the depth (m) of the tank and L is the length (m).

If Q represents the flowrate, W the width of the settling tank, A the horizontal cross-sectional area of the settling tank then we have

$$Q=vW/D$$

Thus

$$v_s=Q/A$$

In an upward-flow settling tank, such as a hopper-bottom clarifier, the key is to make the horizontal cross-sectional area sufficiently big so the upward-flow velocity is significantly less than the settling velocity of the water. In practice the upward-flow velocity is set at approximately half the settling velocity of the floc particles.

In a laminar clarifier a velocity gradient exists for the velocity parallel to the plates.

And sizing of the tank or basing is governed by the equation

$$v_s= vd / (d \sin\theta + L_s \cos\theta)$$

where v_s is the vertical settling velocity(m/s), v is the flowing velocity(m/s) parallel to the plates, L_s is the length(m) of the plates and θ is the angle(rads) of the plates to the horizontal. (Degremont, 1991).

2.6 Filtration

Sedimentation removes the majority of impurities from suspension, but not all. In water treatment, filtration is typically added to further removes particles from suspension in water (Degremont, 1991).

2.6.1 Types of Filtration

The categorization of filters in water treatment vary to a degree. One common categorization is based on the main method of capture of particles.

The rapid sand filter is a common type of filter where water moves vertically through relatively coarse sand and other granular media which capture floc and other impurities, separating them from the water that percolates down. It takes less land compared to filters like the slow sand filter. The filter needs regular cleaning to remove the particles caught in the filtering media. A common method of cleaning is by backwashing, which reverses the direction of water flow. Compressed air is also added during backwashing to aid the process (Degremont, 1991).

The slow sand filter is a type of filter that grows a biological film on the sand. The sand in it only acts as a substrates and does not perform the filtering itself. The filtering is done, instead, by the biological layer called Schmutzdecke, which consists of bacteria, fungi, protozoa rotifer and a variety of aquatic insect larvae. It takes 10-20 days for the Schmutzdeck to fully form in the top few millimetres of the fine sand layer. During those days all water that goes through the filter is not purified properly and goes to waste. The filter also needs to be refurbished after a period as the schmutzdecke grows to a degree that it blocks the water from passing through fast enough. One way to refurbish it is simply to scrape off the schmutzdecke layer to expose the new layer of sand to grow another schmutzdecke. An alternative, called wet harrowing, does it by reducing the water level to just above the schmutzdecke then stirring the sand which precipitates solids in that layer and letting the remaining water to pass down the sand. The natural process does not require much extra energy for pressurizing etc. It is

therefore more suitable for developing countries, though some developed countries apply it in some areas too, like the UK (Degremont, 1991).

Membrane filters are also used to treat drinking water and sewage. They can remove all particles more than 0.2µm in diameter (Degremont, 1991).

2.6.2 Filtration Theory

In general there exist four filtration mechanisms, which are sedimentation, interception, Brownian diffusion and inertia (Degremont, 1991).

Sedimentation separates the settleable particles from the water. The settling velocity depends on factors such as the size, shape and density of the particle, as well as the viscosity of the water.

Interception works mainly on large particles by catching them through gradually reduced pore size.

For particles that are small enough they are under the influence of thermal gradients which cause them to diffuse towards granules in the filtering media. This is called the Brownian diffusion named after botanist Robert Brown who discovered this phenomenon in 1827.

Inertia occurs when large enough particles go off their streamline and bump into media grains.

2.6.3 Pressure Drop

The Kozeny-Carman equation (Degremont, 1991) is one equation used to calculate the pressure drop of fluid that flows through a packed bed of solids.

$$\frac{\Delta p}{L} = - \frac{180 \nu (1 - \epsilon)^2}{\Phi_s^2 D_p^2 \epsilon^3} u_s$$

Where Δp is the pressure drop (Pa); L is the depth (m) of the pack of solids; ν is the viscosity (Pa · s). ϵ is the porosity; Φ is the sphericity of the particles in the packed bed; u_s is the superficial velocity (m/s); D_p is the diameter (m) of the equivalent particle.

This equation only applies for laminar flows (Degremont, 1991). However, this equation does not take into account the fact that the actual path the fluid goes through is not perfectly straight but more tortuous than the depth of the packed bed (Degremont, 1991).

In the thesis *Deep Bed Filtration: A New Look at the Basic Equations* Horner(1986) has in-depth studies on the evolution of the Iwasaki equations which were first come up with by Iwasaki, who first formulated two equations. The first one describes the mass balance

$$u \frac{\partial C}{\partial l} + \frac{\partial \sigma_s}{\partial t} = 0$$

Where u represents the approach velocity(m/s), C the concentration of particles at depth l and time t . σ is the volume of deposited solids per unit of bed volume.

The second one is the kinetic equation

$$\frac{\partial C}{\partial l} = -\lambda C$$

λ being a constant.

A variation of other constants and factors have been added into the equations throughout the years. Specifically with the mass balance equation, an improved and approximated variation is

$$u \frac{\partial C}{\partial l} + (1 - \epsilon_d) \frac{\partial \sigma}{\partial t} = 0$$

ϵ_d is the porosity of the deposit grains.

2.7 Measurement Theory

The water treatment system needs to be fitted with instrumentation to measure various values which are fed into the Arduino microcontroller to adjust the dosing of coagulants as well as the flow rate.

Values to be measured include the flow rate, the pH, the turbidity and the zeta potential.

2.7.1 Zeta Potential Measurement

There are no direct ways to measure zeta potential. Theoretical models are necessary to calculate the zeta potential (Lyklema, 1995).

One way to calculate the zeta potential is through electrophoretic mobility (Lyklema, 1995). An electric field is applied to the dispersion, causing particles to move towards the electrode of the opposite charge with a velocity proportional to the magnitude of their zeta potential. This relationship (Hukel approximation) between the electric velocity and the zeta potential is represented by

$$v_e = \frac{\epsilon_0 \epsilon_r E}{\eta} \zeta$$

Where v_e is the velocity(m/s) of the charged particles, ϵ_0 is the permittivity in vacuum, ϵ_r is the permittivity of the solution, E is the electric field strength(V/m), ζ is the zeta potential(V) and η is the viscosity(Pa · s) of the liquid.

The equation above only applies when the radius of the particle is significantly greater than the distance between the particle's surface to the slipping plane. If the reverse is true, when the radius of the particle is significantly less than the distance between the particle's surface to the slipping plane, the equation (Smoluchowski approximation) is modified by the coefficient $\frac{2}{3}$ as follows (Lyklema, 1995):

$$v_e = \frac{2\epsilon_0 \epsilon_r E}{3\eta} \zeta$$

When the radius and the surface-to-slipping-plane distance are comparable, the coefficient added is between $\frac{2}{3}$ and 1.

The velocity of the particles is measured by a laser beam from a coherent source. The light hitting the moving particles gets scattered, resulting in a frequency shift which is used to indicate the velocity of the particle (Measuring Zeta Potential - EUNCL).

This project uses the streaming potential method. In this method, the electrolyte flows through a chamber where the surface of the chamber is charged, developing a double layer on the surface. This results in a local increase of counter-ions and decrease of co-ions. The movement of the flow generates a current, with a voltage between two electrodes in the chamber. This voltage can be used to work out the zeta-potential with the following equation (REF):

$$\zeta = \frac{\Delta U}{\Delta P} \frac{\eta \kappa}{\varepsilon_0 \varepsilon_r}$$

where the η , κ , ε , and ε_0 are the solvent viscosity (units), conductivity (units), relative dielectric constant (units), and the permittivity of the vacuum (units), respectively (Self-Assembly Processes at Interfaces, Adam West, Interface Science and Technology).

2.7.2 Turbidity Measurement

According to the article-“Measuring Turbidity, TSS, and Water Clarity” (FONDRIEST Environmental Learning Center), measurement of turbidity is liable to be subjective given that it is a qualitative rather than a quantitative measurement.

When measuring the turbidity of water, turbidity is defined as a value proportional to the amount of suspension in it, making it quantified (REF).

Turbidity Units include the Formazin Turbidity Unit (FTU), the Jackson Turbidity Unit (JTU) and the Nephelometric Turbidity Units (NTU) (REF). Standard Arduino turbidity sensors use the NTU as the standard unit (REF).

A widely accepted measurement of turbidity involves a monochromatic source of light which passes through the sample liquid. Suspended particles hit by the light scatter the light which gets received by a detector. The amount of scattered light is proportional to the amount of suspended particles in the sample liquid (REF).

An alternative to measure turbidity is by using a Secchi disk (REF). This is more used when measuring water turbidity in large bodies of water such as a lake, a river etc. In

this measurement, a disk called the Secchi disk is lowered into the water until it is invisible. The depth of the disk when invisible indicates the turbidity.

According to the article *Measuring Turbidity, TSS, and Water Clarity* by the Fondriest Environmental Learning Center (July, 2020), conversion between the NTU and TSS is described by the following equation,

$$NTU = a * TSS^b$$

Where a and b are regression-estimated coefficients, with b approximately equal to 1.

This equation becomes inconsistent, though, when organic material, air bubbles or dissolved coloured material is present. The equation is only suitable when the relationship is relatively linear, when the NTU is greater than 40, a modified, logarithmic equation is often used instead,

$$\log_{10}(SSC) = a * \log_{10}(\text{turb}) + b$$

where SSC is the suspended-sediment concentration in mg/L, turb is the turbidity in formazin nephelometric units, a is a regression coefficient and b is Duan's bias correction factor.

2.8 Control Theory

According to the website *TutorialsPoint*, Control theory is a field dealing with automation of various technological systems whose operation depends on its own operating variables. Control systems are generally divided into open-loop systems and closed-loop systems. An open-loop system is a system where the signal only progresses forward. Consequently the control action is not dependent on the output of the system. Figure 2-11 gives a simple illustration of the open-loop control model.

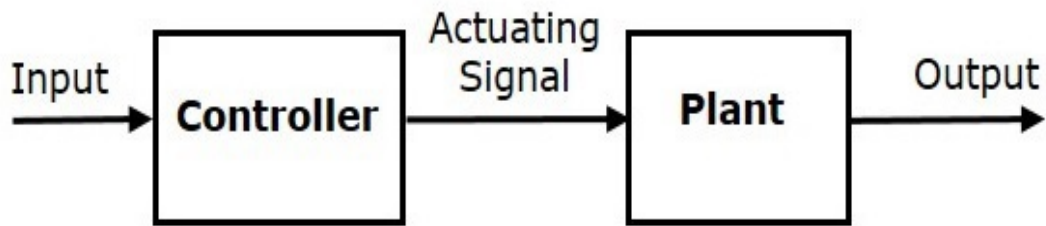


Figure 2-12 Example of an open-loop control system (TutorialsPoint:Control System, July, 2020).

A more studied control system is the closed-loop control system that feeds back the output, either partially or completely, to the input, which makes adjustment according to the feedback (TutorialsPoint: Control System, July, 2020). Figure 2-12 shows the diagram of a closed-loop control system.

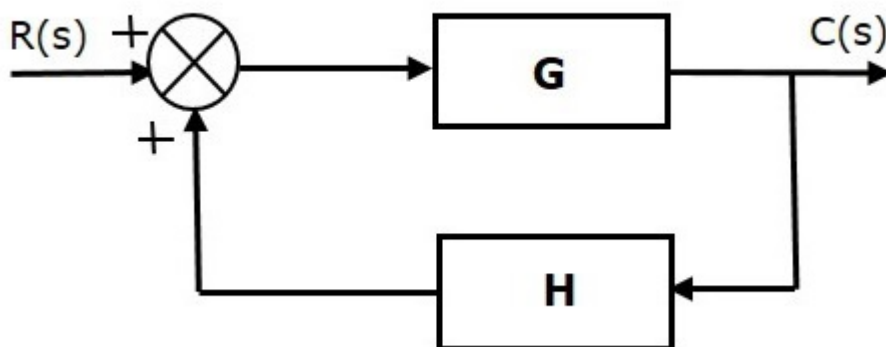


Figure 2-13 A closed-loop control system (TutorialsPoint:Control System, July, 2020).

The closed-loop system is further divided into the positive and the negative control systems (TutorialsPoint:Control System, July, 2020). The main difference between them is described by the following two equations.

Equation for positive open-loop systems:

$$T = \frac{G}{1-HG}$$

Equation for negative open-loop systems:

$$T = \frac{G}{1+HG}$$

Where T represents the transfer function, G represents the open-loop gain, a function of the frequency, and H the gain of feedback path, which is a function of the frequency too.

For a closed-loop control system, the latency is the time delay between the output signal being generated and when it reaches back to the input for the adjustment. The lower the latency, the quicker the reaction of the control system, and the less the error of the process will be.

2.9 Example of Lab-Scale Water Treatment for Teaching

A comparable project has been done by Ma in 2012 from the Michigan Technological University. The project was summarised in the thesis *Design of a lab-scale direct-filtration system and Its Application in Process Lab*. A direct-filtration pilot system was needed for a senior-level engineering class at MTU, for students to gain hands-on experience with water/wastewater treatment technologies. The report included theoretical studies of principles related to water treatment, including the history of water treatment, especially filtration, coagulation and flocculation, and general theory of the filtration system.

Calculations concerning the filtration system size, Reynolds number and the granular bed porosity and the backwash calculation factor were made before the construction of the system.

The building of the system then was performed including the water tanks, rapid mixer along with a filtration column. A control panel was built to place all the valves. Figure 2-13 shows the overview of the complete system.



Figure 2-14 Overview of the direct-filtration system

Lake water first enters the storage tank located behind the system. Bentonite is added into the water to provide some suspended solids for the filtration unit to remove. The contaminated water is then directed into a blue tank (on the left of Figure 2-14) where coagulant is introduced into the water by an FMI pump.

Water then flows first into a settling column for the flocculation process, after which it proceeds into the filtration column for filtration, which is the final stage of treatment. Both the flocculation and the filtration columns look the same, shown in the Figure 2-14 in the middle behind the control panel. After treatment, turbidity meter was used to measure turbidity of the water.

Following the completion of the building of the unit, tests were run through which certain flaws were found and modifications were made to rectify them. Major problems encountered included one failure of the unit, erroneous readings of the water and coagulant flowrates, and unclarity of the operating instruction.

2.10 A Case Study on Arduino for Teaching

A case study was done by two researchers- Kirikkaya, E.B. &Basaran, B, from Cogaeli University on students learning with Arduino technology, their content summarised in the thesis *Investigation of the Effect of the Integration of Arduino to Electrical Experiments on Students' Attitudes towards Technology and ICT by the Mixed Method.*

The researcher made a plan of lab experiments through a time span of 15 weeks, with some experiments running over one week and some over two weeks. Fifty first-year students from Cacaeli University were selected to take the course. For those experiments, an online administrative system was developed for students to preview, review their courseware, and submit their assignments. The course included quantitative analysis along with some quiz questions in the form of an interview for qualitative feedback from the students. The researchers concluded that most students who were not familiar with the Arduino program at the beginning of the course gradually picked it up through the designed experiments. It was also found that most students were not familiar with the Fritzing program, the program the lab used for Arduino development.

1. week	<ul style="list-style-type: none"> • Information to teacher candidates about the applications be made in the laboratory (presentations). • Implementation of pre-tests for TAS and ICT. • Loading of the 1. Experiment sheet to the e-support system.
2. week	<ul style="list-style-type: none"> • 1. Experiment: Beginning of electricity experiments. Introduction of course tools, materials, Arduino and Fritzing programs. • Loading of the 2. Experiment sheet to the e-support system.
3. week	<ul style="list-style-type: none"> • 2. Experiment: Ohm's law, current, voltage, resistance values measured by Arduino. • Evaluation of posters of 1. week. • Loading of the 3. Experiment sheet to the e-support system.
4. week	<ul style="list-style-type: none"> • 3. Experiment: Current, voltage and resistance measurement for series-connected circuits. repeating measurements with Arduino. • Evaluation of posters of 2. Experiment. • Loading of the 4. Experiment sheet to the e-support system.
5. week	<ul style="list-style-type: none"> • 4. Experiment: Measurement of current, voltage and resistance for parallel connected circuits with Arduino. • Evaluation of posters of 3. Experiment. • Loading of the 5. Experiment sheet to the e-support system.
6. week	<ul style="list-style-type: none"> • 5. Experiment: Arduino measurements of resistance, current and voltage in mixed circuits. • Evaluation of posters of 4. Experiment. • Loading of the 6. Experiment sheet to the e-support system.
7. week	<ul style="list-style-type: none"> • 6. Experiment: Kirchhoff rules and applications. • Evaluation of posters of 5. Experiment. • Loading of the 7. Experiment sheet to the e-support system.
8. week	<ul style="list-style-type: none"> • Mid-term exam
9. week	<ul style="list-style-type: none"> • 7. Experiment: Introduction of LED lamps and taking some measuring with Arduino related with flashing LEDs. • Evaluation of posters of 6. Experiment. • Loading of the 8. Experiment sheet to the e-support system.
10. week	<ul style="list-style-type: none"> • 8. Experiment: Potentiometer presentation and measurements; Observation of the potentiometer voltage value with arduino and adjustment of the LED brightness. • Evaluation of posters of 7. Experiment. • Loading of the 9. Experiment sheet to the e-support system.
11. week	<ul style="list-style-type: none"> • 9. Experiment: Introduction of capacitors and various measurements; determination of capacitor capacitance with Arduino. • Evaluation of the posters of the 8. Experiment • Loading of the 10. Experiment sheet to the e-support system.
12. week	<ul style="list-style-type: none"> • 10. Experiment: Charging and discharging of capacitors. • Evaluation of posters of 9. Experiment. • Loading of the 11. Experiment sheet to the e-support system..
13. week	<ul style="list-style-type: none"> • 11. Experiment: Finding the inductance of coils with different windings. • Evaluation of posters of 10. Experiment. • Loading of the 12. Experiment sheet to the e-support system..
14. week	<ul style="list-style-type: none"> • 12. Experiment: Determination of L inductance of a Coil. • Evaluation of posters of 11. Experiment. • Application of attitude tests for TAS and ICT.
15. week	<ul style="list-style-type: none"> • Evaluation of posters of 12. Experiment. • Final exams. • Performing semi-structured interviews.

Figure 2-15 Application Steps in Laboratory Studies

3 Preparation Work on Electronic and Water Treatment Components

Preparation work was performed on the electronic components and the water treatment equipment. Specifically, most electronic components were tested with a simple testing code and certain sensors were calibrated before use. The zeta potential sensor had to be fabricated because of the high cost of devices available on the market. A list of fittings needed to house the sensors and for connecting the water tanks had to be purchased for the installation.

3.1 Theory and Preparation Work on Electronics

The water treatment system is controlled by Arduino which drives the pump to keep the flow of water, the dosing pump which injects alum (potentially other chemicals if needed), receives readings from sensors (pH sensors, turbidity sensors, one zeta potential sensor, flow rate sensors and multiple temperature sensors and particle size sensors), and makes adjustment according to the readings fed into the computer. Figure 3-1 demonstrates the initially planned schematic for the water treatment system.

The yellow cable connected to the gate (middle leg) of the MOSFET transistor controls the amount of current received by the motor with a number between 0, which corresponds to 0% of the current and 255, which corresponds to 100% of the current, with a simple code below.

A more efficient approach is to use a motor driver, as is the case of this project, which uses an L298N Dual H-Bridge Motor Driver, with the schematic shown below.

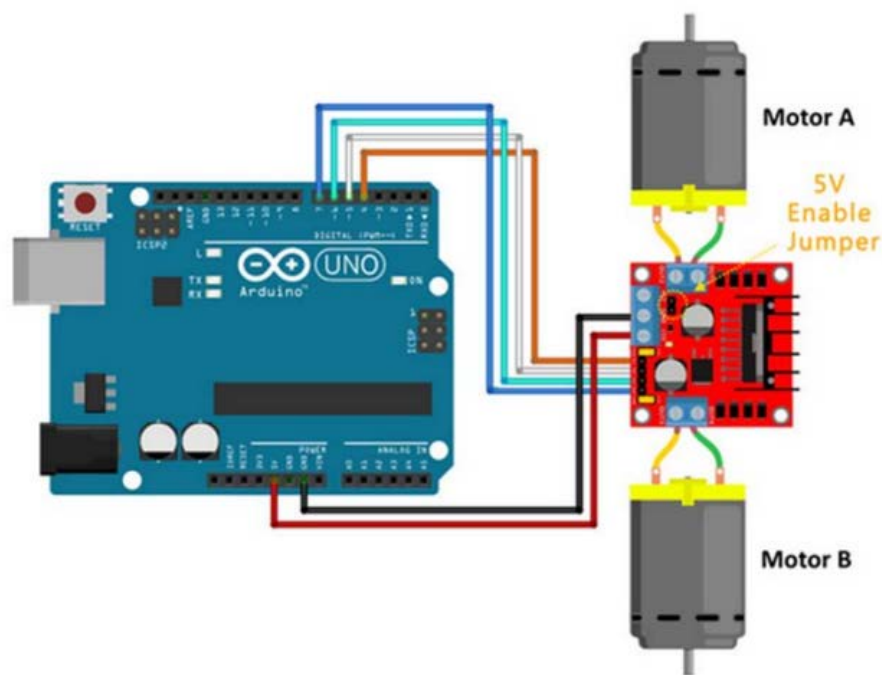


Figure 3-3: Schematic of an L298N Dual H-Bridge Motor Driver (Handson Technology)

Only one motor (water pump) was connected since there was only one water pump needed in the system.

3.1.2 PH Sensor

DFRobot HAOSHI pH electrodes were purchased for use in the water treatment. At least two pH sensors were needed, one to measure the pH value before the clarification process, and one after.

The sensor gives the pH value in linear relation to the voltage generated according to the pH value. The linear equation is represented as

$$y = kx + b$$

where the letter y representing the pH value, and x representing the voltage. With the two-point calibration method, two buffer solutions with known pH values are provided, in this case 4 and 10, respectively. And with two voltages given by the Arduino code, we have two equations with known x and y, to solve for k and b, which gave the relationship between the pH value and the voltage.

The code including the equation with k and b values deriving from the calculation mentioned above is in Appendix A.

3.1.3 Turbidity Sensor

The gravity Arduino turbidity sensors were used for measuring turbidities before and after the purification process, Figure 3-4 shows the sensor.

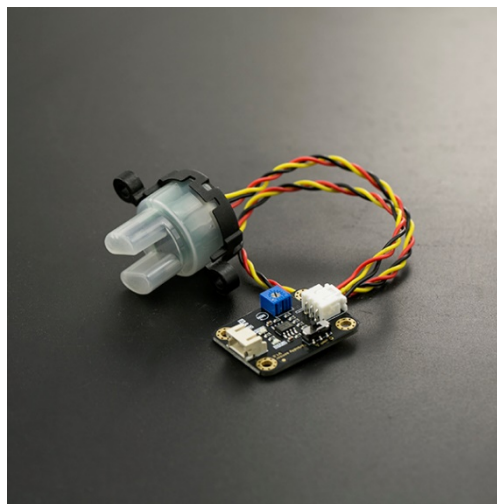


Figure 3-4 Gravity Arduino Turbidity Sensor

The sensors measure the turbidity of a liquid based on light detection. A gap splits the sensor into two probes, one emitting light and the other receiving it. The light

transmittance and scattering rate depend on the suspended solids in the liquid measured which fills the gap between the two probes.

The electronic schematic of the turbidity sensor (TSD-10) is shown in Figure 3-4.

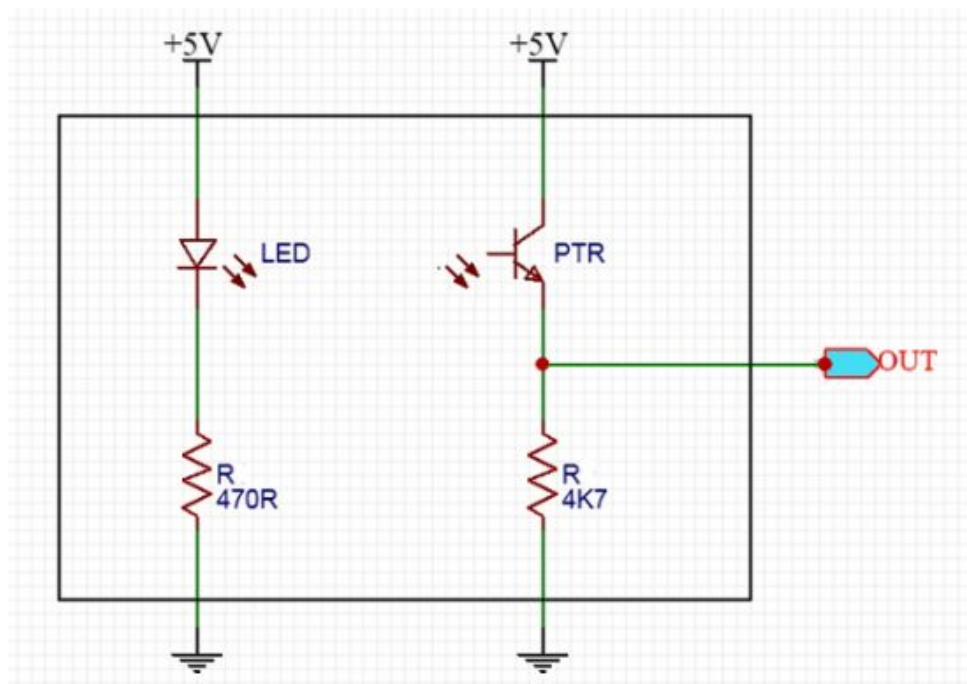


Figure 3-5: Electronic Schematic of the TSD-10 Turbidity Sensor (Electro Schematics)

Calibration of the turbidity sensor is based on the parabolic relation shown in Figure 3-5 (with x representing the voltage, whilst y stands for the pH value).

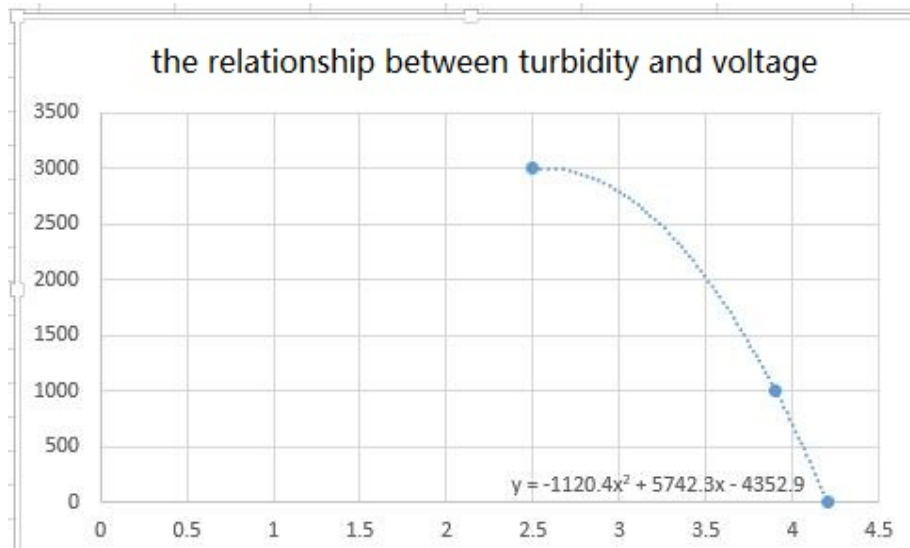


Figure 3-6: the Relationship between turbidity and voltage (Electro Schematics)

The calibration code for the turbidity sensor is also given in Appendix A.

3.1.4 Dosing Pump

Two DFRobot peristaltic dosing pumps were purchased for use in the treatment system. One dosing pump was used for dosing in the alum for coagulation and flocculation. The other was used to adjust the pH value of the sample water. The DFRobot pump is shown in

The dosing pump works on 5-6V with a maximum operating current of 2.5A. Assuming that it would work on 5V, the Arduino internal power supply would be enough, no need to add an external power source.

The pump has a maximum flowrate of 45ml/min. The speed input number ranges from 0 to 180, with 0 and 180 corresponding to maximum flowrates in either direction and 90 corresponding to pump being static, and numbers in between corresponding to speeds between the maximum and 0 speed or flowrate.

A testing code for the dosing pump is given in Appendix A.

3.1.5 Flowmeter

Flowmeters were used to measure flowrates at different parts of the treatment process. A minimum of two were needed, one before the settling tank and one after the filtration.

The YF-S201 Hall Effect Water Flow Sensors were used for the measurement. They could measure between 1 and 30 liters/min, more than enough for the scale of the water system.

The testing code of the flowmeters is included in Appendix A.

3.1.6 Zeta Potential Measurement

Arduino zeta potential sensors are mostly either extremely expensive, difficult to calibrate, or unreliable (Ref). So a simple substitute solution was devised. The measurement would involve the Mutek PCD 03 machine was used with the piston oscillating up and down a sample liquid holding cell similar to the original cell that came with the Mutek machine. Minor modifications were that two holes were drilled into the sides of the cylinder so liquid would continuously flow in and out of the cell, able to reflect the change of the voltage, thus the zeta-potential in the water treatment system.

The measuring cell is shown in Figure 3- 6 .The cell is 50mm wide and 117mm wide.

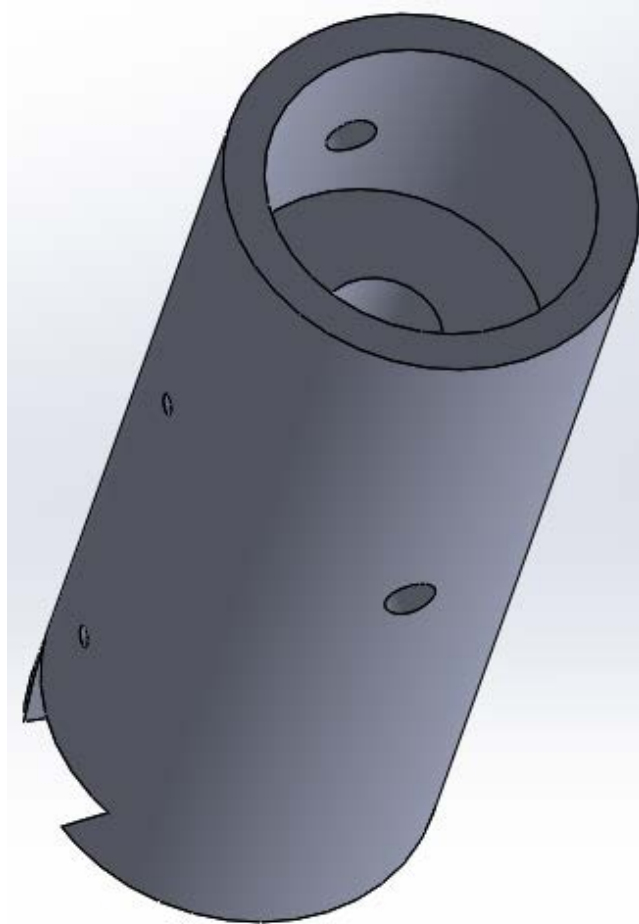


Figure 3-7 Zeta-Potential Cell.

The cell is connected to the Arduino board which measures the voltage, indicating the zeta-potential.

The cell was 3-D printed several times, all with leakage due to the honeycomb structure. A liquid sealant was purchased and applied to the surface of the cell to prevent leaking.

3.2 Water Treatment Components

Components for the water treatment itself were prepared for assembly. These include settling tanks, filtration columns, and various fittings and various other components.

3.2.1 Water treatment tanks

As mentioned in Chapter 2, three tanks are needed to be used to for settling separately- a conventional tank, a hopper-bottom and a lamina. 3-D models of them were generated by SolidWorks, as shown in Figure 3- 7 , Figure 3- 8 and Figure 3- 9 .

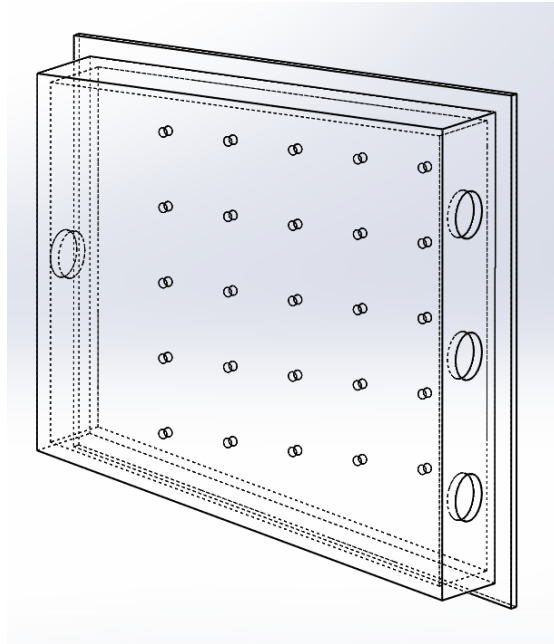


Figure 3-8: Lab Conventional Clarifier

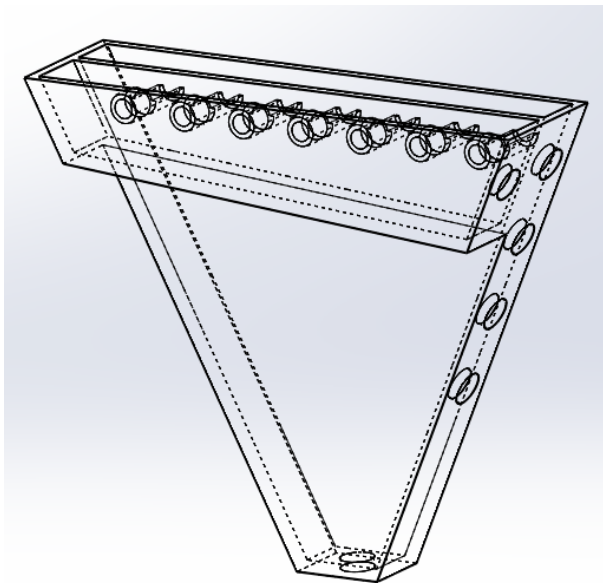


Figure 3-9: Lab Hopper-Bottom Clarifier

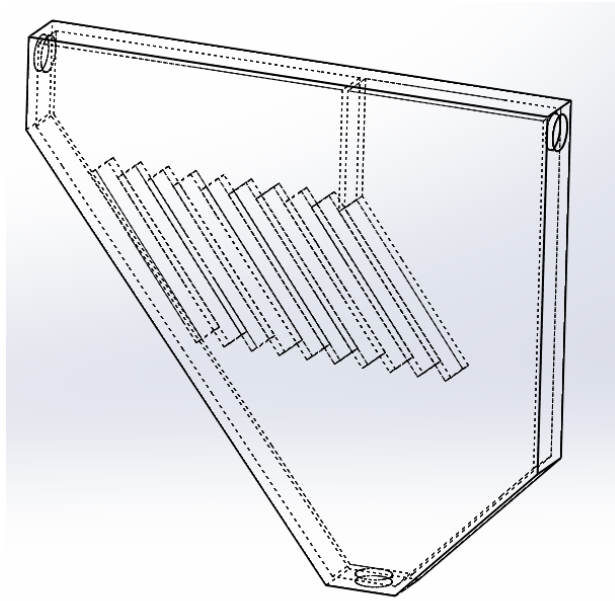


Figure 3-10: Lab Lamina Clarifier

At each experiment, one of them is to be connected in the system before the filtration and after the static mixers.

The details of their working principles were already mentioned in chapter 2. It will therefore not be repeated here.

3.2.2 Filtration Column

After sedimentation, the water flows into the filtration column for further purification. The filtration columns consists of three layers of filtering material, and a backwashing mechanism to clean the filters.

Figure 3-10 shows the 3-D design of the filtration column.

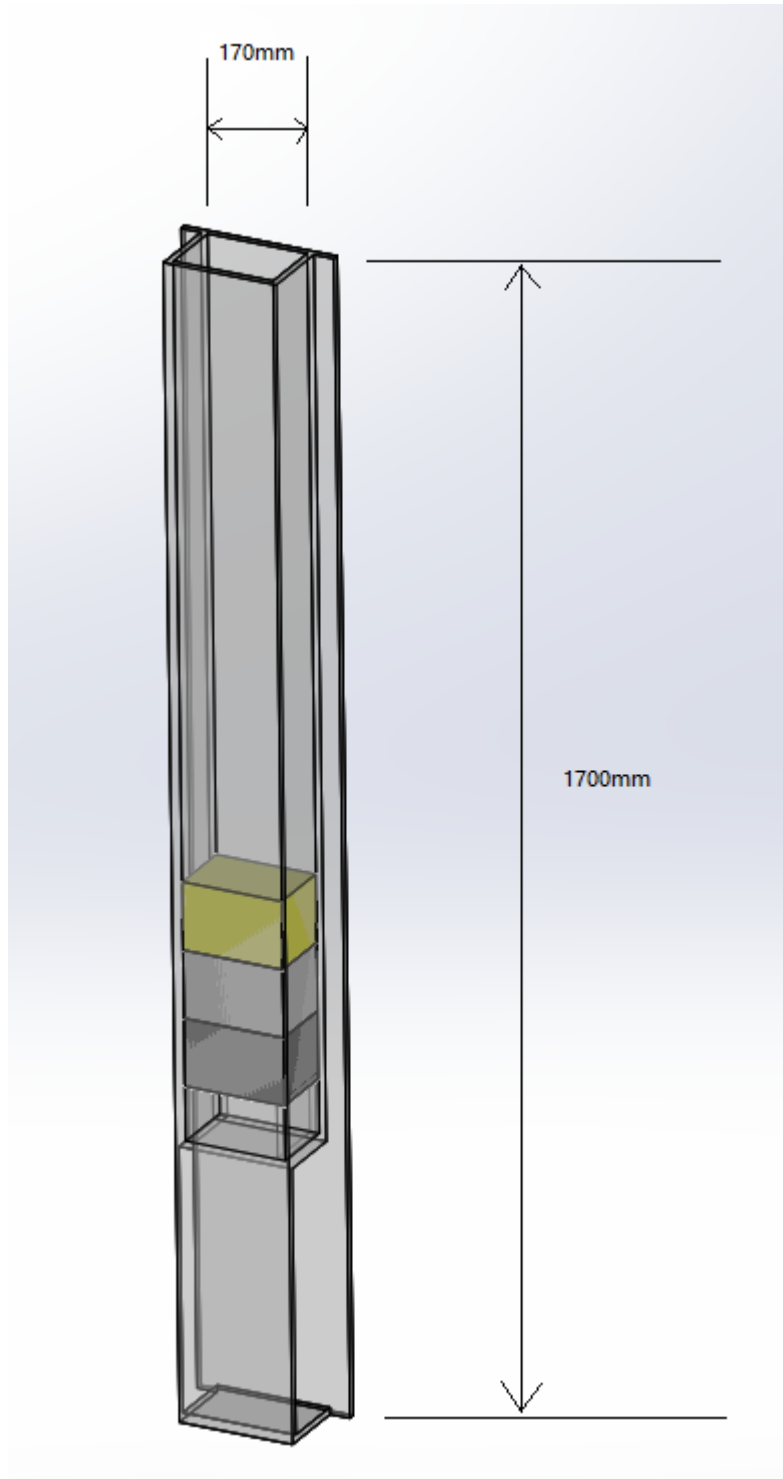


Figure 3-11 Lab Filtration Column

3.2.3 Mixers

3.2.4 Sensor Housings

Two housings were made, each to be fitted with a turbidity sensor and a pH sensor, as is shown in Figure 3-1 1 . The protruding ring fits the pH sensor, whereas the flush hole beside it fits the turbidity sensor. Two bolt holes are made to fix the turbidity sensor.

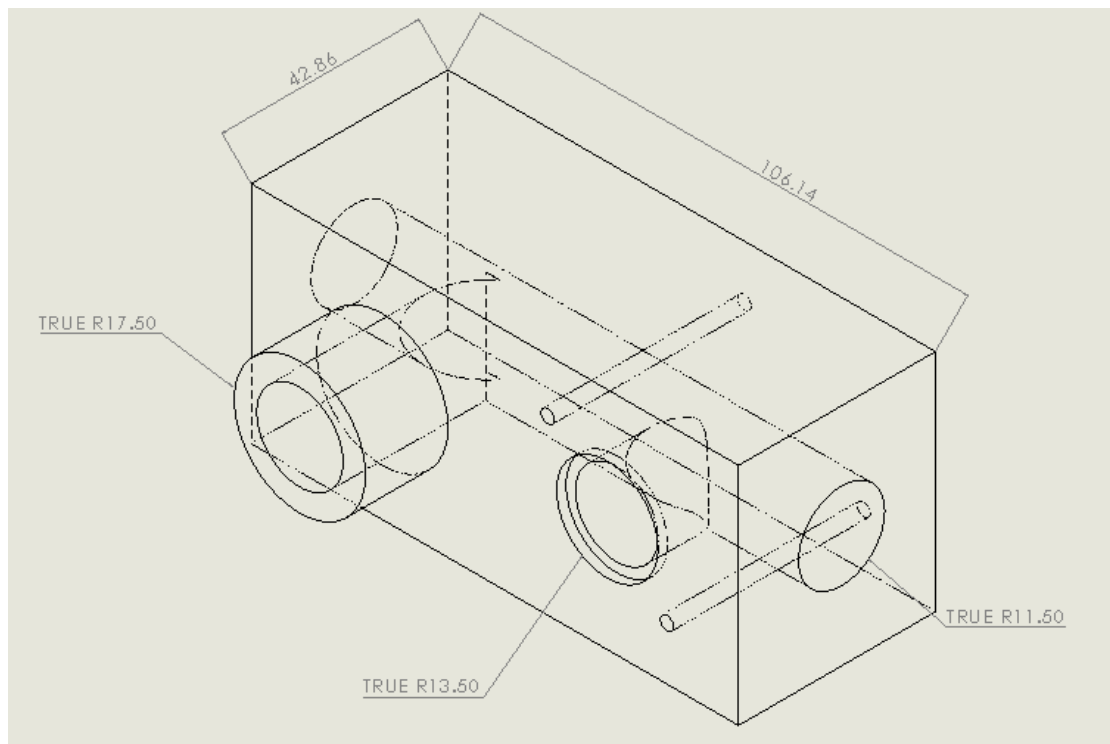


Figure 3-12 Turbidity and pH Housing

4 Initial Assembly

A simple system of one flowrate sensor, one turbidity sensor and one pH sensor working with the Arduino MEGA board was assembled and programmed for a test run to check the coordination between the three aforementioned sensors. The P&ID diagram of it is shown in Figure 4-1.

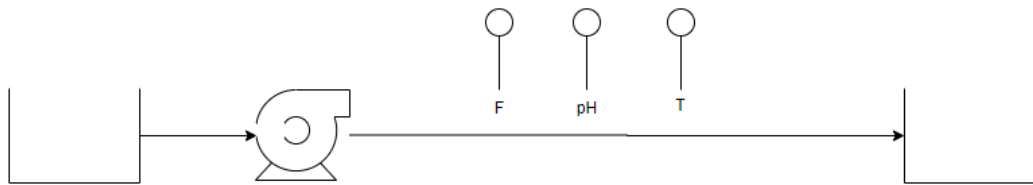


Figure 4-1: P&ID diagram for one of each sensors (flowrate, turbidity and pH)

The flowrate was set at 10L/min and sealant was applied and modifications were made to ensure no leakage was present. The final assembly was not likely to reach a flowrate of 10L/min so if the system could withstand 10L/min then it would be able to withstand the flowrate in the final system.

5 Sensor Calibration

The flow meter, two turbidity sensors, two pH sensors, the zeta-potential sensor and the two dosing pumps all need calibration to give comparatively accurate readings. The sensors provided have limitations in their accuracy and fluctuate in their readings. Consequently it is impractical to calibrate them to perfection. A significant amount error should be expected and to accentuate the purification process it is recommended that the alum for purification should be strong enough to make the turbidity readings before and after the settling significant enough to make the difference sizeable enough for the two sensors to read.

A series of calibration was carried out in the course of two weeks to study and improve the accuracy of the sensors.

5.1 pH Calibration

The principle of calibration of the pH sensors was given in Chapter 3. Nevertheless, the two individual sensors had slight different readings for the same pH buffer solutions. A separate calibration independent of the calibration instruction provided by DFRobot was conducted.

The calibration used three buffer solutions, with pH values 4, 7 and 10 respectively.

Each pH sensor was dipped into those three buffer solutions successively and readings were recorded. Table 5-1 is the readings recorded by pH sensor One.

Table 5-1 Calibration Data of pH Sensor One, showing voltage readings at different times for pH 4, 7, and 10

pH	Voltage Readings at Different Times (V)									Average	Stdev	Stderror	% Error
	1	2	3	4	5	6	7	8	9				
4	1.05	1.08	1.04	1.08		1.25	1.16	1.18	1.1	1.12	0.07	0.03	2.29
7	1.99	1.98	1.97	2		2.07	2	2.13	2.06	2.03	0.06	0.02	0.97
10	2.79	2.78	2.78	2.74	2.78	2.73	2.93	3.02	2.99	2.84	0.11	0.04	1.30

A scatter plot chart was generated based on data provided above, shown in Figure 5- 1

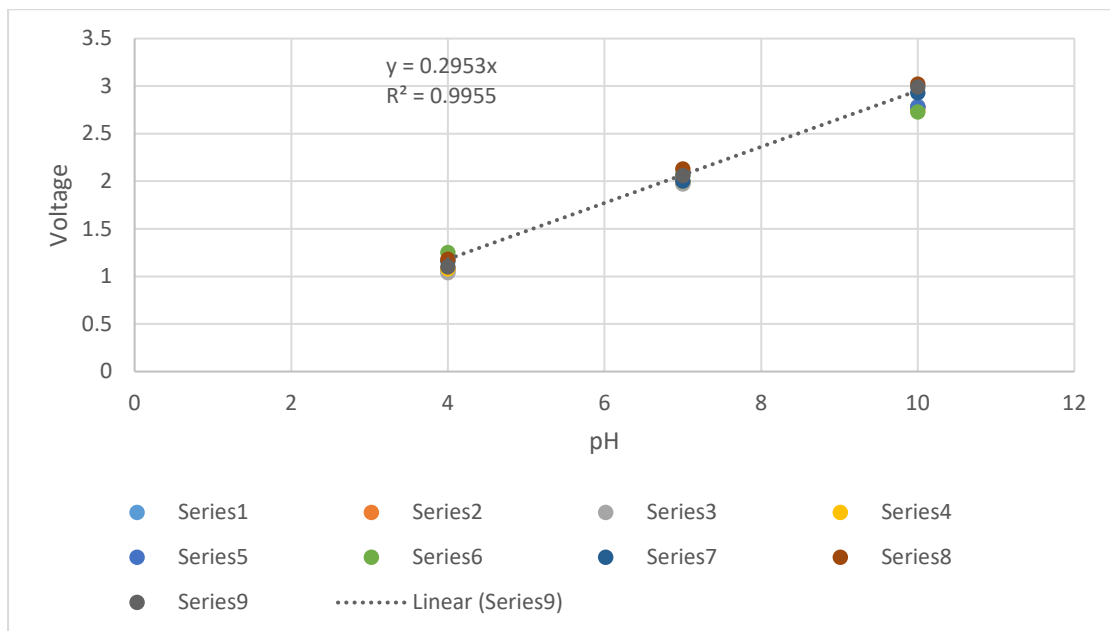


Figure 5-1 relationship between voltage and pH for pH Sensor One

Compared with Sensor One, Sensor Two was relatively more stable and readings were consistent. Therefore less readings were recorded and the calibration process was relatively straightforward.

Figure 5-2 is the readings from pH Sensor Two calibration.

Table 5-2 Calibration Readings from pH Sensor 2

pH	Reading		
	1	2	3
4	0.72	0.72	0.72
7	2.18	2.18	2.18
10	3.56	3.58	3.58

And a simple chart with a linear equation was generated, shown below.

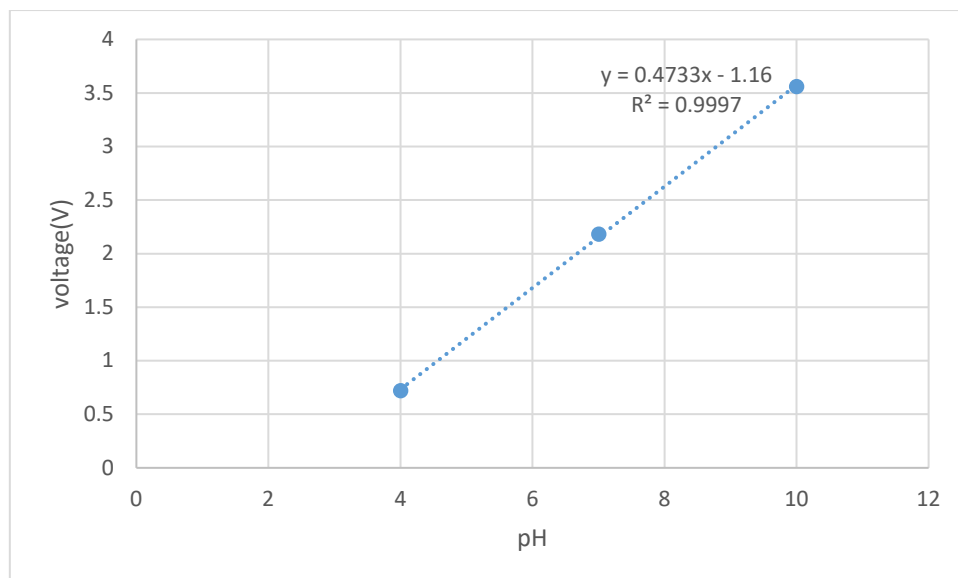


Figure 5-2 Linear Relation between Voltage and pH for pH Sensor Two

5.2 Flowmeter Calibration

Originally two flowmeters were planned for use, one before the dosing and settling and one after the filtration. However, the sensors provided were not sensitive enough to detect the flow at the end of the process which is too slow. So only one sensor was to be used, before the dosing, for the moment.

Calibration was relatively simple. The settling tank was closed and marked where it reaches 5 litres. Then the pump was turned on starting pumping water into the settling tank. The process was timed with a stopwatch until water reached 5 litres. Then

calculation was done working out the flowrate which was compared with the readings of the flowmeter, which was adjusted to match the calculated flowrate.

Table 5-3 Calibration Data of the Flowmeter

Pump Voltage(V)	Flow rate(L/min)	Measured Flow Rate(L/min)		Difference
		max	min	
12	6.8	6.76	6.64	0.12
10.5	5	5.01	4.89	0.12
9	2.5	2.67	2.32	0.35
8	1.5	1.46	1.23	0.23
8	1.25	1.32	0.9	0.42
8	0.9	1	0.57	0.43

As is shown in the table, the overall trend is that the lower the flowrate, the higher the error. It is therefore inadvisable to set the flowrate too low. For the system installed in the lab specifically, the safe range of the flowrate is rather narrow in the first place, so the value of the acceptable flowrate should not be a significant problem.

For the power setting of the pump, it is not recommended that the voltage should drop below 9 volts, which would cause significant error, or rise above 12 volts, which would cause the settling tank to overflow very quickly.

5.3 Turbidity Calibration

This was the hardest and most unreliable part of the calibration process. The DFRobot turbidity meters were highly unreliable with their default readings. Every start of a new run of the programme gave a different reading ranging between 2.0 volts to 4.75 volts.

A series of calibration efforts have been attempted, with new turbidity sensors purchased to test if a difference would be detected. None achieved stable readings that could be relied upon.

5.3.1 Attempt One

The first calibration attempt was conducted by measuring a range of kaolin solutions with turbidity values measured from 0 to 598. The DFRobot turbidity sensor was then programmed and used to measure each of the samples.

The figure below shows the data obtained from the attempt.

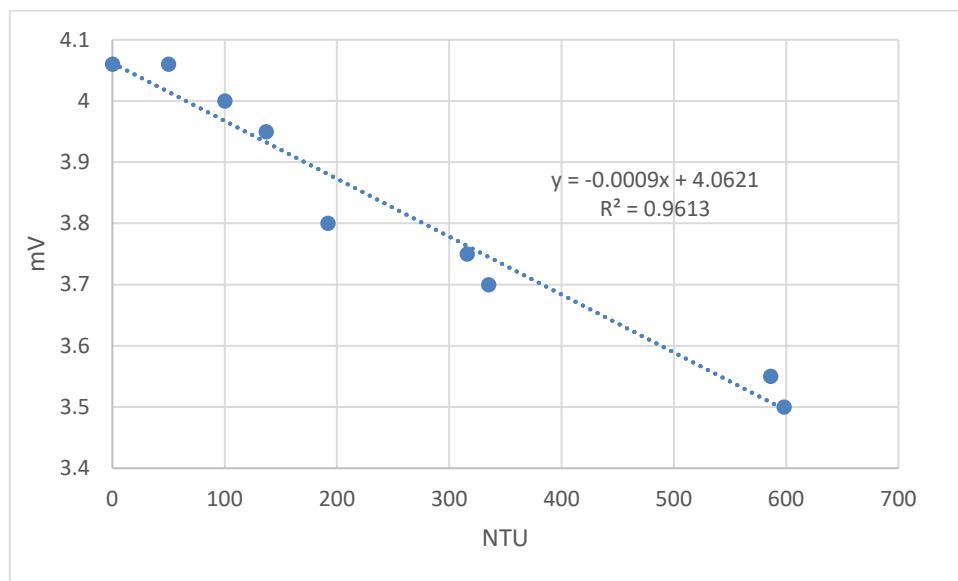


Figure 5-3 Turbidity Voltage Readings VS NTU

This calibration was deemed unreliable due to the instability of kaolin solutions, which gave unreliable NTU values to begin with. Instability of kaolin arises from that the kaolin suspension gradually settles with time, so the turbidity decreases with time.

5.3.2 Attempt Two

Attempt one was conducted several months before the final run of the system, with the assumption that the sensors would stay stable after the calibration, which was an incorrect assumption. By the time the system was set up for running, the previous calibration results were no longer reliable, necessitating another calibration. The trend

continued with further calibration from this point on and will be shown with data given in later attempts.

The second calibration was carried out several days before the final run of the system.

The approach was slightly different to address certain flaws detected from the first calibration effort.

One major flaw out of control of the experiment was the instability of the lab turbidity sensor itself, as will be shown later with the data collected (in Table 5-5 for example, sample one's turbidity ranges from 105 to 139, a difference of 34). To address this, different concentrations of soap water were made. And each sample was measured by the same lab turbidimeter several times, instead of only once, to approximate a comparatively accurate turbidity value of the samples.

And two turbidity sensors were run at the same time to make sure they were close enough in their readings, as opposed to the first calibration effort where different turbidity sensors were calibrated separately, at different times. The results of the calibration were given in Table 5- 5 and Figure 5- 4 .

Table 5-4 Calibration Data for Turbidity Sensors (Attempt Two)

Sample	Measured Values by Lab Turbidimeter											Average	Average Sensor Voltage Reading	
1	105	122	104	126	103	118	139	114	117	119	119	117	116.9167	4.2
2	436	451	460	447	445	437							446	3.7
3	987	1000	976	1000	1000								992.6	3.3

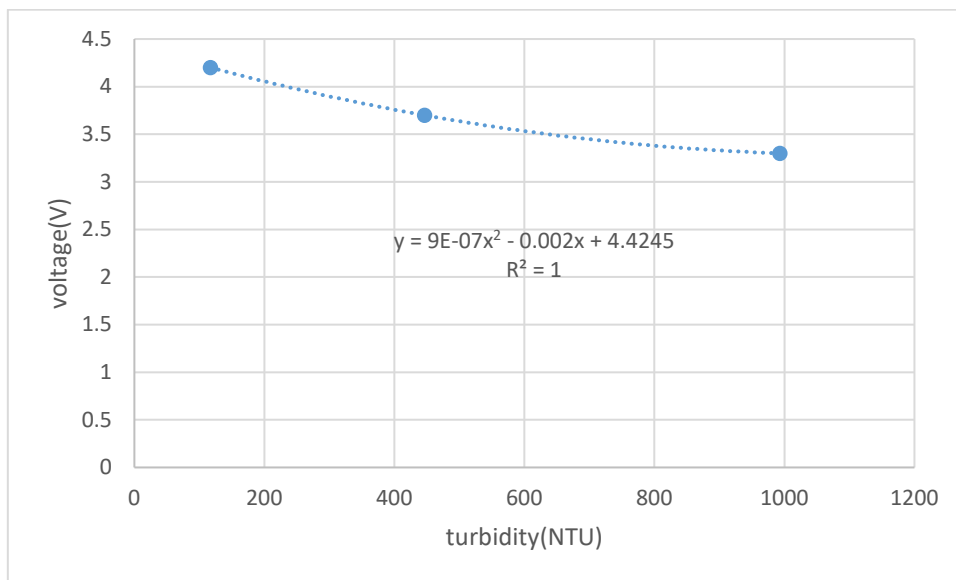


Figure 5-4 Voltage VS Turbidity for Turbidity Sensors' Calibration

5.3.3 Calibration of dosing pumps

The dosing pumps' speed is controlled by a speed input ranging from 0 to 180, with 0 corresponding to the maximum speed counter-clockwise, 90 to stop and 180 to maximum speed clockwise.

Flow rates at different speeds of the pumps were measured to work out an approximate relation between the numerical input into the Arduino controller and the flowrate. Table 5-6 shows the data collected.

Table 5-5 Calibration Data for Dosing Pumps

Arduino Input	flow rate(mL/min)
180	27
170	25
160	21
150	16

One important discovery from the simple test is that the pump does not rotate, therefore operate at all, with an input below 150, giving a very limited range of working flowrates of the dosing process. The concentration of the solution will therefore precisely match the range of the working flowrates to efficiently implement the flocculation and coagulation processes.

Figure 2- 1 shows the relation between the speed input and the flowrate

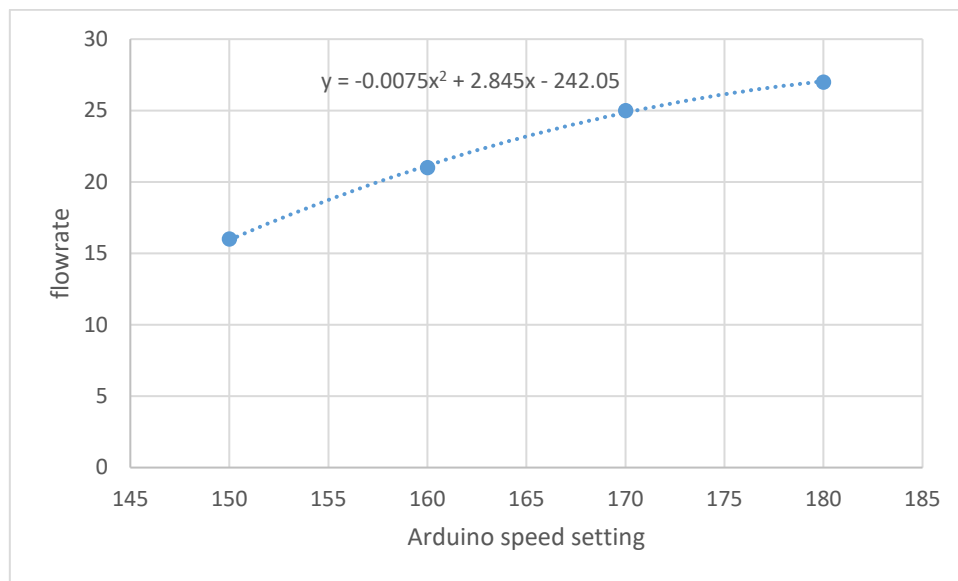


Table 5- 1 Relation between Arduino Speed input and Dosing Flow Rate

5.3.4 Jar Tests

In addition to calibration of electronic components, a series of jar tests were performed to work out the optimal coagulation dose.

A jar test is used for determining the optimum coagulation dose. According to the lab instruction given by the Environmental Lab of University of Waikato, 0.2g/L kaolin suspension is used. 6 jars each contain 1 litre of water. 6 doses of aluminium sulphate solution of 1g/L are to be prepared, with volumes of 5, 10, 20, 25, 35 and 50 mL respectively. They are to be added into each sample being stirred by agitators at 100 rpm for 3 minutes. After 3 minutes each sample should be slowed down to 30 rpm. After 10 minutes the agitators should be turned off and another 5 minutes should be taken for the samples to settle. Then each sample's turbidity is to be measured and the relationship between turbidity and dose is to be plotted according to the data.

Flocculation first occurred at 3:30, 30 seconds after the agitation speed was turned from 100 rpm to 30 rpm.

The data of the first performance was given in Table 5- 8 and Figure 5- 5 .

Table 5-6 Jar Test Result One

0.2g/L Kaolin Jar Test Result						
1g/L Al ₂ SO ₄ (mL)	5	10	20	25	35	50
Turbidity (NTU)	7.99	9.76	3.04	2.03	1.69	1.06

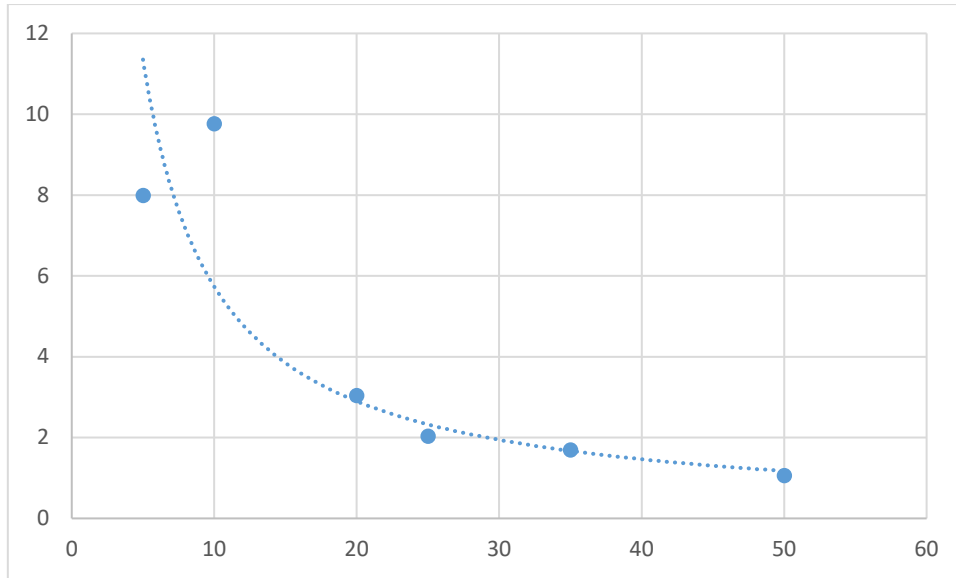


Figure 5-5 Aluminium Sulphate Dose VS Turbidity

However, Figure 5-5 shows an abnormality with the second datum, suggesting there could have been mistakes that introduced inaccuracy into the process.

So a second test was conducted for more reliable data, and additional caution of measurement and timing was taken.

The process was almost the same except that the kaolin samples were mixed separately in each jar instead of made in one batch then poured into each jar separately as was done in the first test.

Data from the second test was given in Table 5-8 and Figure 5-6 .

Table 5-7 Second Test Result

0.2g/L Kaolin Jar Test Result						
1g/L Al ₂ SO ₄ (mL)	5	10	20	25	35	50

Turbidity(NTU)	10.4	9.06	2.27	1.55	1.46	1.18
Zeta Potential(mV)	-268	-290	-290	-290	-270	-280

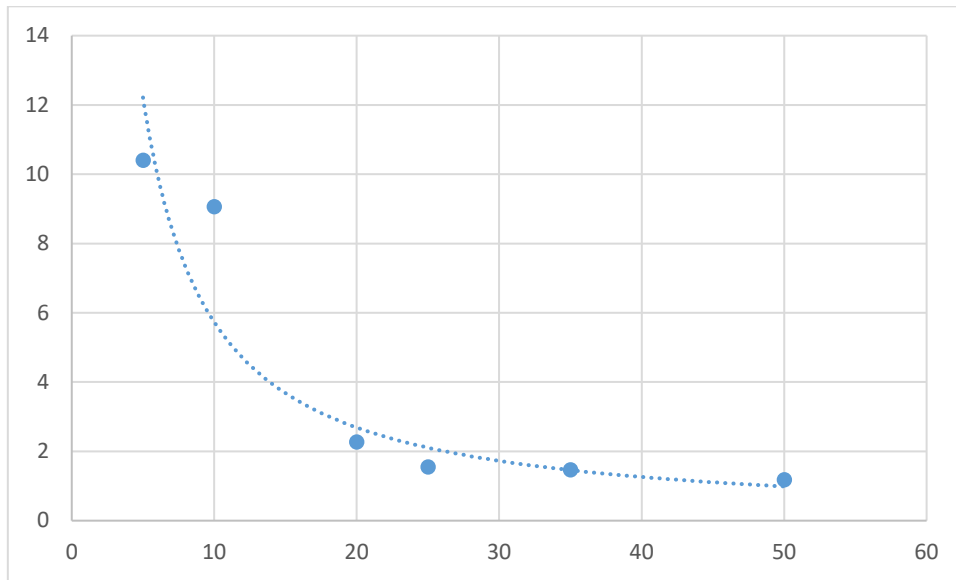


Figure 5-6 Second Test Result Plot

From the second test results, it seems that except one aberration on datum two in the first result, the overall trend does match up for both tests. The turbidity decreases overall with the increase of aluminium sulphate dosage. And it decreases the most between 10mL and 20mL of aluminium sulphate solutions, after which it continues to decrease but increasingly slower.

A third test ensued with modified aluminium sulphate concentration, 1.5g/mL this time.

This time floc started forming at 3:00 due to the increased concentration of aluminium sulphate. Tabulated and graphic results are given below.

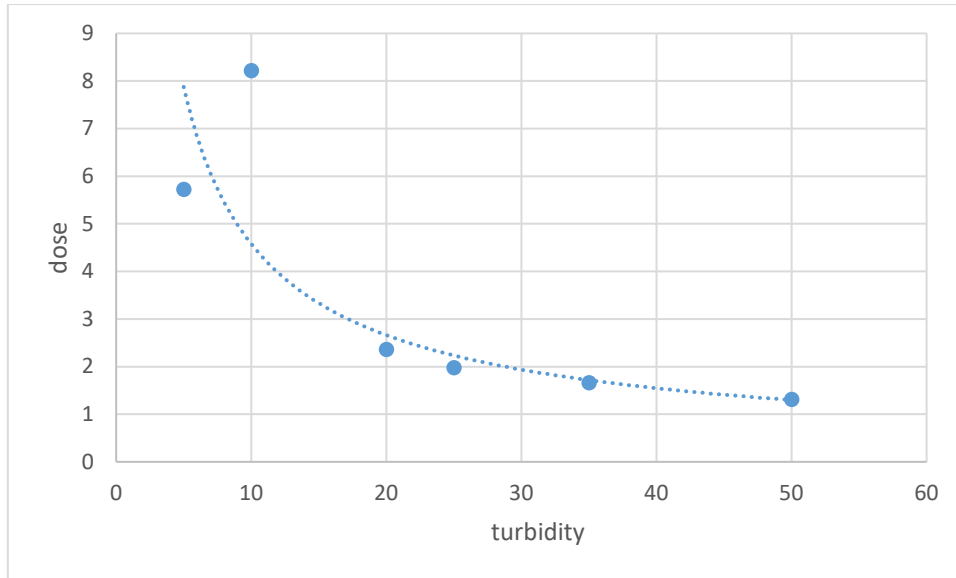


Figure 5-7 Third Jar Test Graph

Again, the turbidity keeps decreasing, without giving the optimum dose. Therefore another more test was carried out with the aluminium sulphate concentration raised to 2g/L this time. Results are given below.

Table 5-8 Fourth Jar Test Result

2g/L Al₂SO₄ VS 0.2g/L Kaolin Suspension						
Al ₂ SO ₄ Solution(mL)	5	10	20	25	35	50
Turbidity(NTU)	34.9	6.19	1.62	1.82	4.64	25
Zeta Potential((-1)*mV)	240	250	284	282	265	210

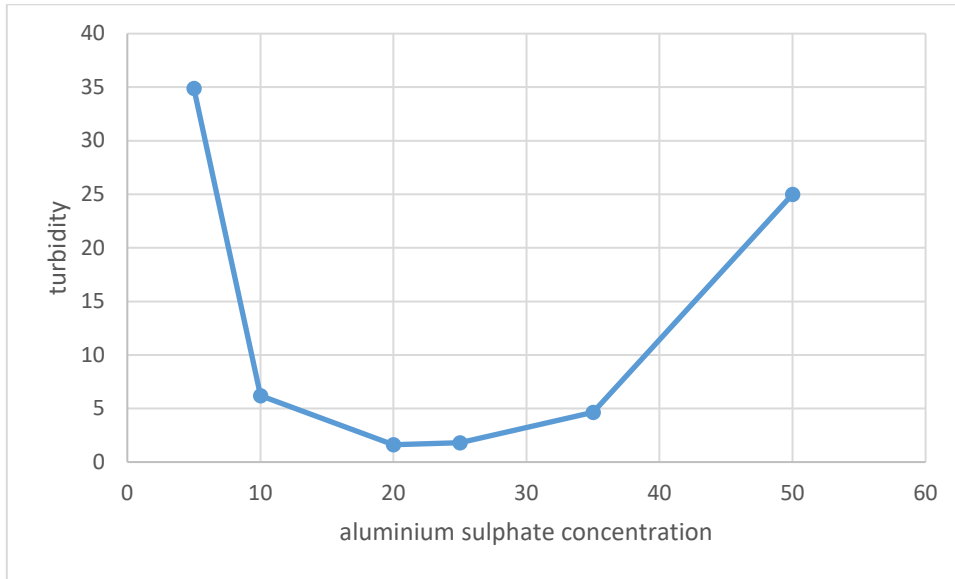


Figure 5-8 Jar Test 4 Turbidity Plot

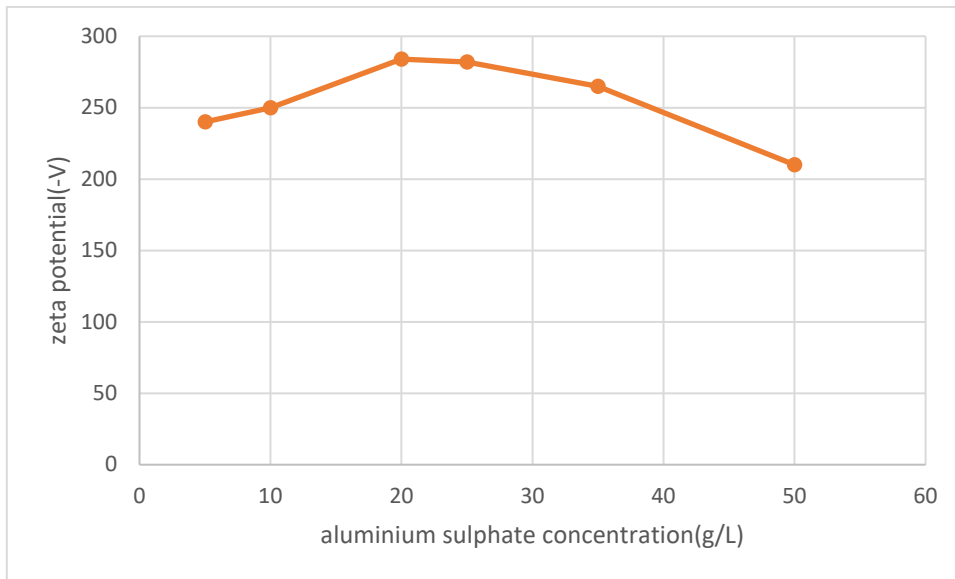


Figure 5-9 Jar Test 4 Plot Zeta Potential VS $Al_2(SO_4)_3$ Concentration

This time it showed the result expected, namely a minimum turbidity in the middle both before and after which it rises above that value. And that point, in this case with 20 mL of 2g/L $Al_2(SO_4)_3$ solution mixed with one litre of 0.2g/L kaolin suspension, the

optimum mixing rate is achieved, and the mixing rate ideally should be the mixing rate for the $\text{Al}_2(\text{SO}_4)_3$ solution for flocculation in the final water purification system.

6 Final Assembly and Tests

6.1 Final Assembly

The water treatment components were assembled together and connected to electronic sensors. Certain modifications were made compared with the initial schematic in Figure 3-1. The new schematic is shown below in Figure 6-1.

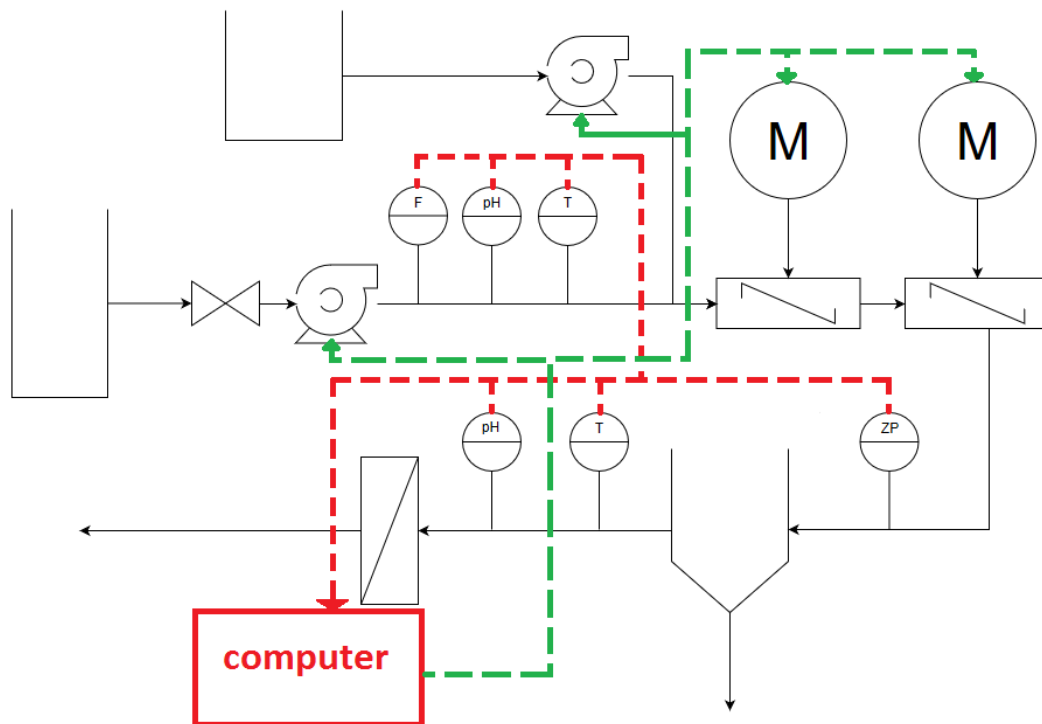


Figure 6-1 Final Assembly Schematic

Compared to the initial schematic in Figure 3-1, the pressure sensors were removed to simplify the coding and Arduino work. The turbidity sensor at the end of the process was removed too given that the sensors are mainly meant to reflect change during the flocculation and coagulation process instead of the filtration process.

The final assembly of the water treatment system includes a water container to store the sample water, an impeller to agitate the sample water, two sensor housings to fit a turbidity sensor and a pH sensor each, a settling tank, with the hopper-bottom, laminar and conventional tanks taking turns for experiments, and a filtration column loaded

with three filtering layers. Details of the clarifiers and the filtration column were already given in Chapter 3.

The water storage container is just a regular cylindrical container with a storage capacity of 90 litres of water, as is shown in Figure 2-1, with a motor driver driving an impeller to keep the turbidity consistent.



Figure 6-2 Sample Water Container

6.2 Test Runs with the Hopper Bottom Clarifier

A couple of test runs were conducted with data, mainly the turbidities manually measured to ensure that the system was making a difference with the turbidity. Different flocculants with varying concentrations were tried as well to determine the optimum concentration and the best chemical.

6.2.1 Test Run One

A test run was conducted with no electronics involved just to test the water treatment system would work smoothly.

The water container was filled to its maximum of 90L. Then 3.6 g of kaolin was added into it, giving it a concentration of 0.2 g/L.

A major problem detected in this run was that there is not enough retention time for floc to form in the settling tank during the process. As mentioned in calibration, the lowest flowrate detected by the flowmeter is 0.9L/min. With the settling tank's (hopper-bottom) capacity at around 8L, it gives roughly 9 minutes for the settlement process. Which, in this test, was not enough. Figure 6-3 shows the sample water after half an hour in the settling tank. As is shown in the photo, the turbidity is still visible after half and hour.

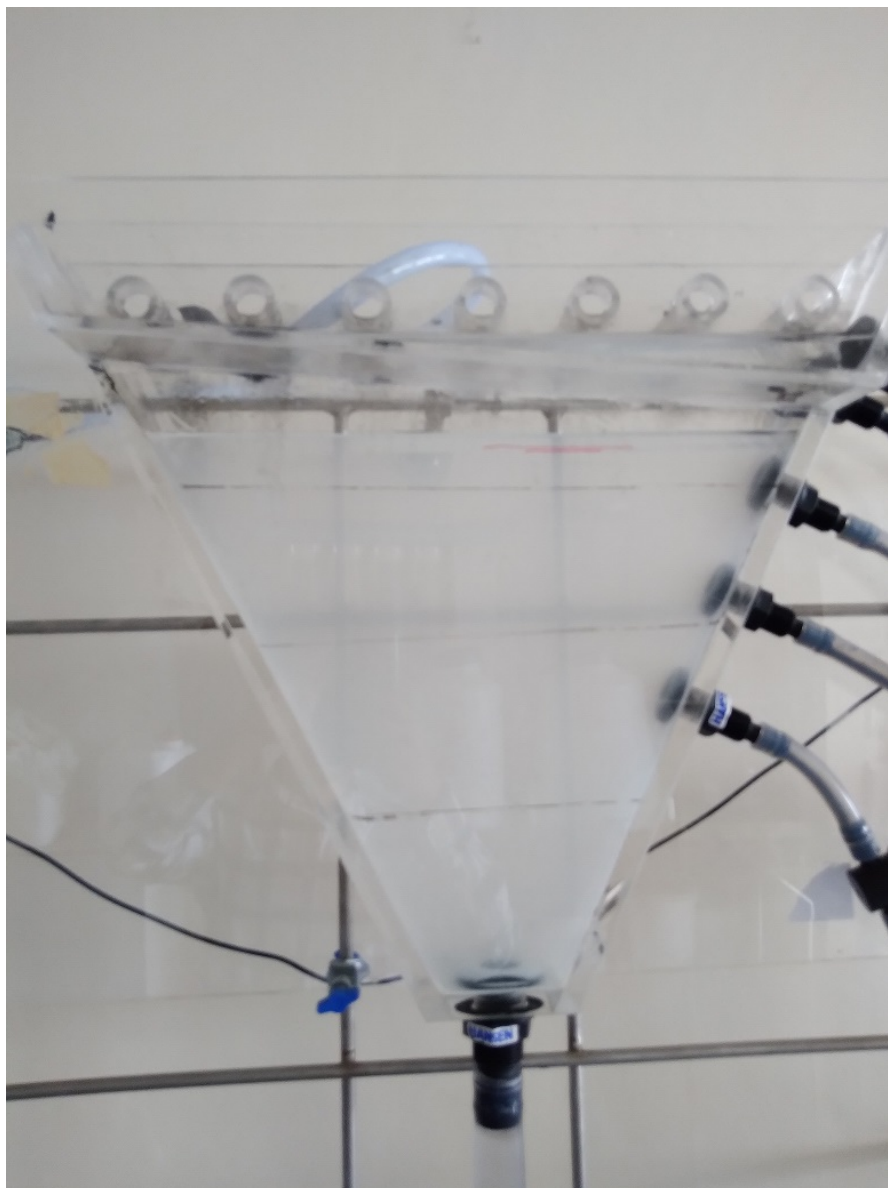


Figure 6-3 Sample Water After 9 Minutes in Test Run One

To determine exactly how much time was needed for the water to become visibly clearer. The tank's drainage was closed up and 5 litres of sample water with 0.2g/L kaolin was pumped into the tank. Then 100mL of $Al_2(SO_4)_3$ was added into it and manually mixed. One hour later there was little change. Only after 3:00, over two hours later did the clarity become visible.

Further compromises had to be made for the system to work properly. First, the flowrate had to be reduced significantly to increase settling time in the settling tank, too low for the flow meter to measure. Consequently, the original design to let the Arduino code adjust the dosing pump based on the reading of the flowmeter had to be abandoned since the flowrate would be too slow to generate a reading from the flowmeter.

For the next run, the dosing rate would be set at 180 Arduino speed, the maximum dosing rate, at a constant, instead of being adjusted by Arduino automatically.

6.2.2 Second Run

A second run was conducted, with the flowrate and turbidities at the beginning, after settling and after filtration measured manually to check the clarification results. pH values and the zeta potential were ignored for this run.

The dosing chemical was 2g/L $Al_2(SO_4)_3$ with the maximum dosing rate, approximately 27 mL/min according to Table 5- 6. The result is given in Table 6-1.

Table 6-1 Flowrate and Turbidities measured for Run 2 of Hopper Bottom Clarifier.

Data of Hopper Bottom Run 2	
Flowrate(L/min)	0.13
Turbidity 1(NTU)	216
Turbidity 2(NTU)	116
Turbidity 3(NTU)	1.6

According to the table, clarity was dropped by half after the settling, and further clarified to near perfection after the filtration process.

6.2.3 Test Run Three

For this run, 1.8 litres of 2 g/L of crystal floc was made instead of aluminium sulphate. Almost every other condition was the same as the previous one.

The turbidity measured before settling, after settling and after filtration are given in Table 6-2.

Table 6-2 Flowrate and Turbidities measured for Run 3 of Hopper Bottom Clarifier.

Data of Hopper Bottom Run 3	
Flowrate(L/min)	0.13
Turbidity 1(NTU)	220
Turbidity 2(NTU)	95
Turbidity 3(NTU)	5

The table shows similar results with test 2. The turbidity dropped by approximately half after settling and became almost completely clear after filtration.

A major problem encountered during this run was that the filtration column was blocked from the last run. And no backwash was performed in between. And a further consequence was that as water built up to a height the side of the column burst and water started leaking out, as shown in Figure 6-4 .

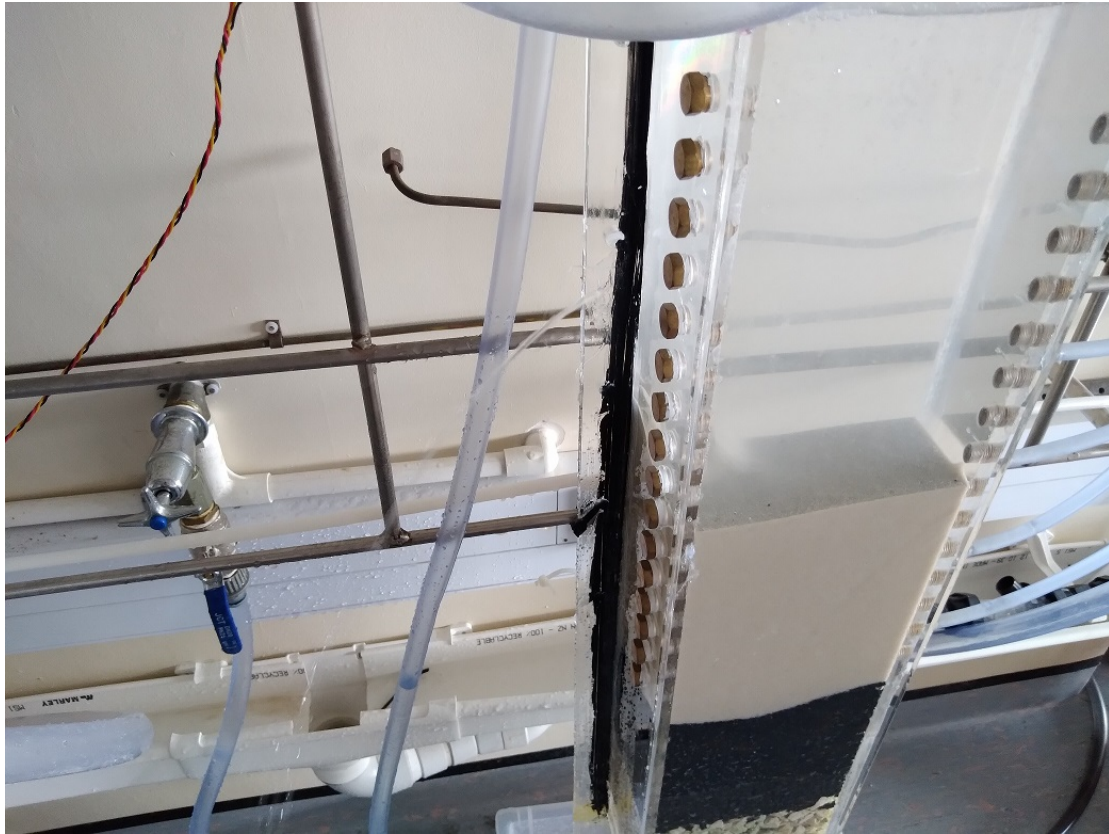


Figure 6-4 Filtration Column Leaks

To fix this, silicon sealant was applied to the side with the leaking. This would temporarily fix the problem. For a long term fix, advisably a more robust column should be made in place of the current one shown in the photo.

6.2.4 One More Calibration

As mentioned in the calibration part, the sensors, especially the turbidity sensors and the pH sensors fluctuate irregularly with time so it is necessary to recalibrate them periodically.

With the turbidity sensors, the first sensor before settling reads 4.33 V for clear water, 4.15 for 128 NTU and 4.33 for 250 NTU, as is shown in

Table 6-3 Turbidity VS Voltage

Turbidity (NTU)	Voltage (V)
0	4.33
128	4.15
250	4

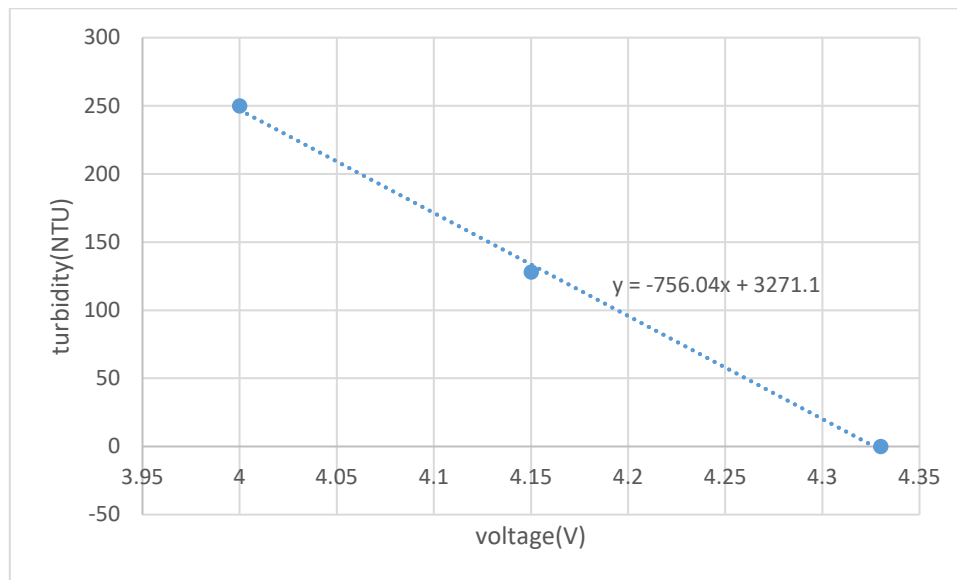


Figure 6-5 Turbidity VS Voltage

And since the turbidity is going to be within 300 and 0, given that the sample liquid is 0.2g/L kaolin suspension, a linear relation is presumably acceptable for this stage of the experiment.

For pH sensors, the first one before settling reads 1.64 for the pH 7 buffer solution and 1.44 for pH 4. This gives a pair of linear equations which when solved gives the relationship between the pH and the voltage reading.

Table 6-4 pH VS Voltage

pH	Voltage (V)
7	1.64
4	1.44

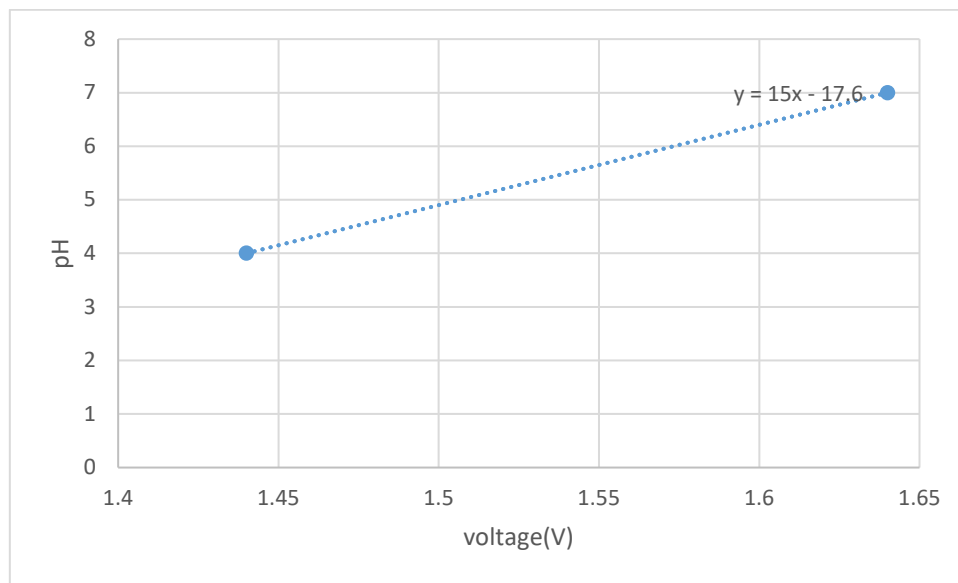


Figure 6-6 pH VS Voltage

Relationship between reading and pH of the second sensor is shown as follows.

Table 6-5 pH VS Voltage

pH	Voltage (V)
7	2.2
4	1.87

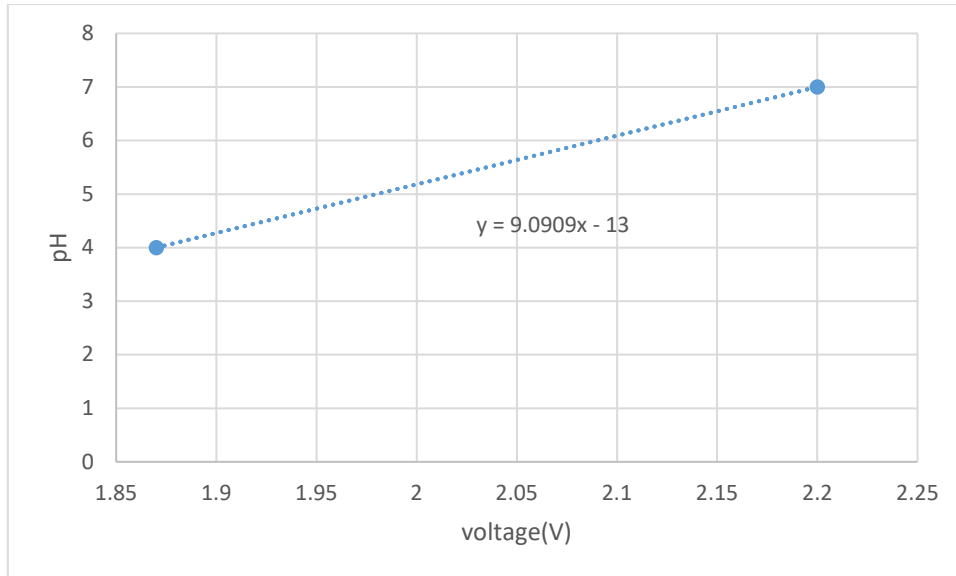


Figure 6-7 pH VS Voltage

As mentioned before, the readings for both the turbidity and pH sensors change constantly so recalibration needs to be performed regularly to ensure an accurate enough reading for all those sensors.

6.3 Final Operation Plan

The final operation involves running the whole system under different conditions, with varying turbidities of samples, varying concentrations of flocculants and varying flowrates, through each of the three settling tanks----the hopper-bottom, conventional and lamina.

6.3.1 Calibration

As shown before, the pH and Turbidity sensors' voltage readings, based on which the pH and turbidity values are calculated, are unstable, changing with time constantly. It is therefore recommended that a calibration should be conducted right before the beginning of the run of the system to maximise the accuracies of the sensors.

For the calibration of the pH sensors, as has been done before, a linear equation is adopted to represent the relation between the voltage reading and the pH value, as follows:

$$y = a x + b$$

where y represents the pH value and x the voltage reading from the sensor. The constants a and b are to be calculated based on two voltage readings from two buffer solutions with known pH values. With a and b worked out, the relation between the pH and the voltage is known.

The linear relation is only accurate within a certain range of pH and does not represent the relation between the pH and the voltage accurately when measuring a pH value far removed enough from the two values of either buffer solutions. Examples of previous calibration efforts show that when buffer solutions of pH values 4 and 7 are used for calibration, the result of reading buffer solution with pH 10 ranges from 9.5 to 10.5, roughly 0.5 different from the actual value.

According to the public article *Effect of pH on the flocculation behaviours of kaolin using a pH-sensitive copolymer* by Shulei Li (2016), Kaolin suspensions flocculate at an optimum within the pH range of 3 to 6. Therefore, the calibration is preferably to use buffer solutions with pH values 4 and 7, with the pH value 10 solution as an optional testing solution to test the accuracy of the values.

For the turbidity sensors, the recommended relation between the NTU value and the voltage value is a parabolic relationship, mathematically represented by equation:

$$y = a x^2 + b x + c$$

where y is the NTU value and x the voltage reading from the sensor.

However, after a series of calibration efforts, it is clear that this relation is highly inaccurate, partially because the constant a , b and c are extremely high values in their thousands, leading to an enormous error with even a small voltage value. It is therefore recommended that a linear equation should be used instead provided that the NTU values of sample water are within the range accurately represented by the linear equation, as has been done in the previous calibration in this chapter.

For a linear relation at least two NTU values need to be known to work out the constants a and b in the equation

$$y = a x + b$$

but since the proper relation is supposed to be a parabolic relation instead of linear, three values are to be taken rather than two to ensure the linear relation approximation is within an acceptable margin of error.

With the kaolin suspension in the container currently at a concentration of 0.2g/L, and clear water an obvious solution with NTU value of 0, another in-between value could easily be attained by dilution a glass of 0.2g/L kaolin sample, providing a third reference value between the 0.2g/L (approximately 225 NTU) and clear water.

With three values, it is unlikely that all three of them are perfectly lined up in a linear relation. The relationship should, as a consequence, be derived by an Excel graphic representation with the trendline representing the approximate relationship between the turbidity and the voltage reading from the sensor.

6.3.2 Operating Conditions

The plan is to run the system under different varying conditions. Tentatively there are four variables in the operation: (1) the concentration of the kaolin sample, consequently its turbidity, (2) the strength of the flocculant (crystal floc or aluminium sulphate) with different concentrations, (3) the flowrate and (4) the settling tank used for the sedimentation process.

With the concentration of kaolin, at least two concentrations were planned to be tested for each run with all other conditions the same, with an optional third test out of the range of turbidity sensors(0.2g/L) to see if the turbidity sensors would still perform well with the linear relation. The three concentrations are as follows:

0.2g/L

0.1g/L

0.5g/L(optional).

Then the strength of the flocculant. Again, at least two concentrations of flocculant should be made, one according to the optimum result of the jar test, 2g/L for both

$\text{Al}_2(\text{SO}_4)_3$ and crystal floc, one slightly higher, and an optional extra one slightly lower, as follows:

2g/L

3g/L

1g/L(optional).

And if feasible and time allows, both flocculant solutions should be tested with other conditions remaining the same in the system.

Then for the flowrate, to give enough settling time for the flocculation the flowrate is preferably to be set as low as possible. The flowrate needs to be above 0.15g/L to be detected by the flow sensor so preferably the flowrate should be set as close to that as possible.

And finally the settling tanks should take turns one after another for the sedimentation with other conditions remaining the same.

The planned order of operation is to operate two runs one right after another with only the flowrate varied since it's the easiest to alter, then alter the dosing concentration which is the second easiest, then the concentration of kaolin, and finally the settling tanks.

In total, at least 2 x 2 x 3 runs are to be performed with their turbidities before and after the settling, pH values before and after the settling, the flowrate and the zeta potential right before the settling taken for analysis.

And due to the fluctuation of the turbidity and pH sensors the runs should be packed together in as short a span of time as possible.

6.3.3 Precautions

Between each two runs, the settling tank should be cleaned properly to remove all settled floc before the next run begins to ensure that the residual floc in the tank does not contaminate the sample water for the next run to corrupt the turbidity measuring.

Backwashing needs to be performed after each run to remove contaminants in the filter. When water level goes high enough it could burst the side of the filtration column, causing certain leaks. It is therefore advisable to apply sufficient sealant in advance to strength the side where it is vulnerable to pressure.

Some leaking through this system is inevitable, especially at parts where fittings are fitted to hoses. If possible, the hosing should be pushed as far back as possible towards the wall so water would drip onto the trough underneath it. Where that it not feasible, the floor should be mopped regularly to prevent accidents.

In case recalibration is necessary, sealant needs to be reappplied where the sensors are fitted into the flowing circuit, caution needs to be taken to avoid spraying the sealant into the electronic board of the turbidity sensors, which could damage the sensors electronic parts.

It might be difficult for the flowrate to remain stable, due to the decrease of water level in the container and, at the start, the rise of water level in the settling tank, as Figure 6- 8 shows. Since the pump is manually operated, regular adjustment of the voltage from the power supply is necessary to maintain an approximate steady flow of the system. The adjustment should be based on the reading of the flowmeter.

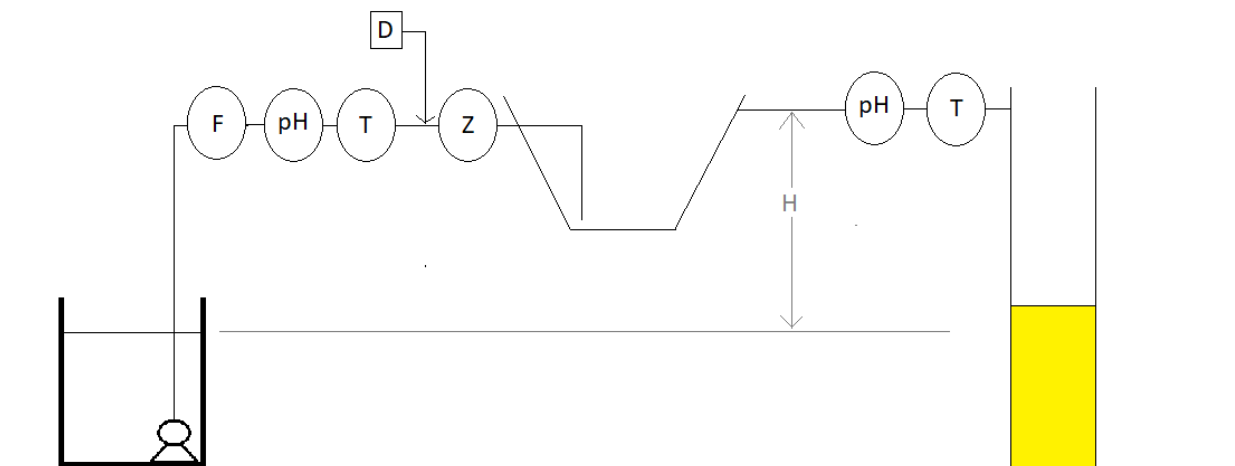


Figure 6-8 schematic of the assembly illustrating the height difference

6.4 Final Tests and Results

Due to the limitation of time, the accidents that occurred when running the system, the final tests were curtailed to only running the hopper-bottom settling tank.

Aluminium sulphate was first used as the flocculant. Five tests were run and recorded.

All turbidity and pH values were manually measured due to the inaccuracy of the sensors and because of the limitation of time another calibration effort of the sensors was not affordable.

All tests were supplied by 0.2g/L kaolin suspension.

In all the following tables, the NTU and pH values measured manually were marked with M1 and M2, with M1 indicating the beginning and M2 after the settling stage. The readings of the pH sensors and the turbidity sensors were included in the table, marked NTU 1, pH 1, NTU 2 and pH 2. The readings were inaccurate when compared to manually measured pH and turbidity readings.

For the dosing pump speed setting, the maximum speed was applied throughout all experiments due to the malfunctioning of the dosing pump. Slow speed settings would often result in the pump getting stuck, putting the dosing process to a halt. The maximum speed corresponds to 180 in the Arduino program.

The first run was completed with 2g/L of aluminium sulphate as flocculant, based on results of jar tests done previously. The details are shown in the table below.

Table 6-6: Results of run one using 0.2 g/L kaolin and 2 g/L alum solution

Time (hr:min)	Before the settling tank								
	Manual					Sensors			
	NTU (M1)	pH (M1)	Water Level(mm)	Pump Voltage (V)	Flow (L/min)	NTU(1)	pH(1)	Flow Rate (L/min)	Zeta Potential
1:22	235	7.44	600	8.6	0.48	472	9.1	0.5	-263
1:36	259	7.33	530	8	0.67	466	8.9	0.57	-190
2:02	258	7.2	490	8.8	0.60	528	8.7	0.28	-208
2:30	251	7.23	390	8.9	0.60	552	8.7	0.5	-190

After the settling tank				
Sensors		Manual		
NTU (2)	pH (2)	NTU (M2)	Flow (L/min)	pH (M2)
981	6.77	213	0.40	6.96
1220	7.19	204	0.32	6.7
1303	7.13	165	0.40	6.9
1438	6.89	236	0.40	6.7

The main goal of the system was to reduce turbidity. As shown in NTU(M1) and NTU(M2), the turbidity was not reduced significantly.

The second run was done the same day, with the flocculant concentration changed to 1g/L. Results are shown in Table 6-7.

Table 6-6 Results of Run Two

Before the Settling Tank								
Time	NTU(M1)	pH(M1)	Water Level(mm)	Pump Voltage	NTU(1)	pH(1)	Flow Rate(L/min)	Zeta Potential
3pm	235	7.24	600	8	607	8.4	1	202
3:20pm	291	7.37	510	8.2	622	8.29	0.4	197
3:50pm	241	7.43	470	8.9	638	8.38	1.12	205
4:00pm	270	7.48	380	8.9	665	8.67	0.797	220

After the Settling Tank										
NTU(M2)	pH(M2)	NTU(2)	pH(2)	pre-fill volume(mL)	pre-fill time(s)	H1	H2	H3	post-fill volume	post-fill time
235	6.95	1511	7	100	9	410	540	600	0	0
246	6.89	1567	6.93	100	33	570	600	610	0	0
217	7.03	1628	6.85	100	6.9	570	600	610	0	0
229	6.96	1653	7.13	100	8	570	600	610	0	0

Still, the NTU did not change significantly between NTU(M1) and NTU(M2).

The zeta potential from both runs were rather high, ranging from -190 to -260, indicating the flocculant did not reduce the repelling charges in the sample to facilitate the coagulation and flocculation process.

Three more tests with different concentrations of aluminium sulphate were done, all of which had little difference in turbidity change. And correspondingly. Results of the three runs are shown in Table 6-8, Table 6-9 and Table 6-10.

Table 6-7 Results of Run Three

Before Settling Tank (Concentration: 0.2g/L, Dosing Concentration: 4g/L)								
Time	NTU(M1)	pH(M1)	Water Level(mm)	Pump	NTU(1)	pH(1)	Flow Rate(L/min)	Zeta Potential (mV)
10:30am	216	7.41	550	9	748	8.26	0.5	-110

After Settling Tank										
NTU(M2)	pH(M2)	NTU(2)	pH(2)	pre-fill volume(mL)	pre-fill time(s)	H1	H2	H3	post-fill volume(mL)	post-fill time(s)
210	7.03	1642	6.58	100	14	50	260	250	100	13

Table 6-8 Results of Run four

Before Settling Tank(Concentration: 0.2g/L, Dosing Concentration: 2g/L)								
Time	NTU(M1)	pH(M1)	Water Level(mm)	Pump Voltage(V)	NTU(1)	pH(1)	Flow Rate(L/min)	Zeta Potential(V)
1:22pm	235	7.44	600	8.6	472	9.1	0.5	-263
1:36pm	259	7.33	530	8	466	8.9	0.57	-190
2:02pm	258	7.2	490	8.8	528	8.7	0.28	-208
2:30pm	251	7.23	390	8.9	552	8.7	0.5	-190

After Settling Tank										
NTU(M2)	pH(M2)	NTU(2)	pH(2)	pre-fill volume(mL)	pre-fill time(s)	H1	H2	H3	post-fill volume(mL)	post-fill time(s)
213	6.96	981	6.77	210	26	0	0	0	100	15
204	6.7	1220	7.19	100	9	0	0	0	70	13
165	6.9	1303	7.13	100	10	200	300	350	100	15
236	6.7	1438	6.89	100	10	410	540	600	100	15

Table 6-9 Results of Run Five

Before Settling Tank(Concentration 0.2g/L, Dosing Concentration(g/L))								
Time	NTU(M1)	pH(M1)	Water Level(mm)	Pump Voltage	NTU(1)	pH(1)	Flow Rate(L/min)	Zeta Potential (V)
2:05pm	260	7.36	600	8	852	8.18	0.5	-60

NTU(M2)	pH(M2)	NTU(2)	pH(2)	pre-fill volume(mL)	pre-fill time(s)	H1	H2	H3	post-fill volume(mL)	post-fill time(s)
230	6.65	1790	5.87	100	21	60	350	290	100	26

Table 6-10 Results of Run Six

Before Settling Tank(Concentration:0.2g/L, Dosing Concentration: 8g/L)								
Time	NTU(M1)	pH(M1)	Water Level(m m)	Pump Voltage	NTU(1)	pH(1)	Flow Rate(L/m in)	Zeta Potential (V)
3:51pm	260	7.36	600	8	846	8.18	0.3	67

After Settling Tank										
NTU(M2)	pH(M2)	NTU(2)	pH(2)	pre-fil volume (mL)	pre-fil time(s)	H1	H2	H3	post-fil volume(mL)	post-fil time(s)
246	6.78	1812	5.87	100	25	60	350	290	100	31

The following day, crystal flocculant was used to replace aluminium sulphate, with concentrations of 2g/L, 1g/L and 4g/L respectively. Their results are shown in Table 6-11, Table 6-12 and Table 6-13.

Table 6-11 Results of Run Seven

Before Settling Tank(Concentration:0.2g/L, Dosing Concentration: 2g/L)								
Time	NTU(M1)	pH(M1)	Water Level(mm)	Pump Voltage	NTU(1)	pH(1)	Flow Rate(L/min)	Zeta Potential (V)
4:40am	2577	7.39	600	8	826	8.21	0.3	67

After Settling Tank										
NTU(M2)	pH(M2)	NTU(2)	pH(2)	pre-fil volume(mL)	pre-fil time(s)	H1	H2	H3	post-fil volume(mL)	post-fil time(s)
125	7.37	1794	6.02	100	25	60	350	290	100	31

Table 6-12 Results of Run Eight

Before Settling Tank(Concentration: 0.2g/L, Dosing Concentration: 1g/L)								
Time	NTU(M1)	pH(M1)	Water Level(mm)	Pump Voltage(V)	NTU(1)	pH(1)	Flow Rate(L/min)	Zeta Potential(V)
10:50am	245	7.36	600	8	1015	8.65	0.5	-32
2:28pm	245	7.36	450	8.5	999	8.54	0.65	-32

After Settling Tank										
NTU(M2)	pH(M2)	NTU(2)	pH(2)	pre-fil volume(mL)	pre-fil time(s)	H1	H2	H3	post-fil volume(mL)	post-fil time(s)
94	7.5	1757	7.08	100	10	0	0	0	100	12
67	7.46	1797	7.41	100	13	40	280	250	100	26

Table 6-13 Results of Run Nine

Before Settling Tank(Concentration: 0.2g/L, Dosing Concentration: 3g/L)								
Time	NTU(M1)	pH(M1)	Water Level(mm)	Pump Voltage()	NTU(1)	pH(1)	Flow Rate(L/min)	Zeta Potential (V)
3:10pm	228	7.54	600	8	1015	8.59	0.4	0
4:00pm	228	7.54	500	8.5	1002	8.41	0.5	0

NTU(M2)	pH(M2)	NTU(2)	pH(2)	pre-fil volume(mL)	pre-fil time(s)	H1	H2	H3	post-fil volume(mL)	post-fil time(s)
152	7.53	1778	7.66	100	12	0	0	0	100	12
139	7.51	1797	7.8	100	12	0	0	0	100	11

Clearly the results improved with crystal flocculant compared with aluminium sulphate. And as the tables show, the optimum clarification is achieved with 2g/L crystal flocculant. On average, zeta potentials of all three runs were lower than with aluminium sulphate.

7 Conclusion

7.1 Modifications from original plan

As already shown from previous chapters, the completed project deviated significantly from the original plan. Here is a brief summary of the major modifications from how it was originally intended

1. The dosing is adjusted manually by the operator instead of adjusted automatically based on the feedback of the flowrate and the turbidity. The main cause of this was that the flowmeter is not accurate enough to read extremely slow flowrates and the system mostly has to operate at low flowrates for enough time for sedimentation in the tank. And consequently the originally planned flowrate sensor for the dosing flowrate was abandoned as well due to its inability to read low values of flowrates and irrelevance given that the flowrate is to be manually adjusted anyway.
2. The 3D-printed zeta-potential cell modelled after the Mutek PCD 03 cell, shown in Figure 3- 6 , did not work, reading only zero throughout the process. Therefore, the original cell provided by Mutek was used. Given that it did not have the inlet and the exit. To drain it, a tray was placed under the Mutek instrument and a hose was inserted into it to drain the excessive liquid into the water trough.
3. Due to leaking issues, only the hopper-bottom clarifier was run and tested. The other two clarifiers, the conventional clarifier and the laminar clarifier could be run and tested with the same principle as the hopper-bottom clarifier.
4. Due to the limitation of time, the system was run without accurate readings from the turbidity sensors and the pH sensors. Several calibration efforts were attempted with data provided in this thesis, mainly in Chapter 5. However, the pH and turbidity sensors were highly unpredictable in their changes of readings and had to be recalibrated almost every time for a new running. Therefore, in the final experiments turbidity and pH values were measured manually with lab

turbidity meters and pH meters. For proper use of the system, sensors could be calibrated according to the correct readings from the lab meters.

7.2 Major issues encountered

As already mentioned in previous chapters, several unexpected issues were encountered throughout the experiment and some of them significantly hindered the process of the experiment. Here are the major ones:

1. The sensors, especially the turbidity sensors and the pH sensors, were highly changeable and had to be recalibrated frequently. Which was time consuming. Preferably better sensors should be used for more accurate and steady readings of turbidity and pH values of the system.
2. Leaking occurred at several places, at various times throughout this experiment. The worst leaking happened mainly at the filtration column when water level went high enough, breaking the sealant applied at the corners of the column. This was shown in Figure 6-4 . As a consequence, sealant had to be re-applied rather frequently, and time had to be taken for the drying before the system could be operated again.
3. The settled floc would pollute the settling tank, contaminating the next experiment. For better accuracy, the tank needs to be cleaned after each individual experiment.
4. The dosing pump is often stuck, not operating smoothly according to the goal. Hence, it had to be set at the maximum speed to facilitate the spinning of the motor. And even so, the pump had to be manually turned several times at the beginning of the operation to start the pumping.

References

- Methods of Water Treatment Ancient to Modern* (2021). Retrieved June, 2020, from <https://www.tlcannon.com/nooash/page.php?c929e7=methods-of-water-purification-ancient-to-modern>
- Hamilton City Council (2010). *A Guide to Hamilton's Water Supply---River to the Tap*. Hamilton, New Zealand. 4p. <https://www.hamilton.govt.nz/our-services/water/water/Documents/A%20Guide%20to%20Hamilton%E2%80%99s%20Water%20Supply.pdf>
- Bratby, J. (2016). *Coagulation and Flocculation*. (3rd ed.). London : IWA Publishing
- McNaught, A. D. & Wilkinson, A. (1997). *Compendium of Chemical Terminology* (2nd ed.). Oxford, U.K.: Blackwell Science.
- American Water College. (2018). *Coagulation Chemistry Basics*, Retrieved 20 July,2020, from <https://www.americanwatercollege.org/water-treatment-coagulation-chemistry-basics/>
- Stratiflo. (n.d.). *Principles of Operation*. Retrieved 20 July, 2020, from <https://statiflo.com/about-static-mixing-2/principles-of-operation/#:~:text=The%20main%20mechanism%20in%20laminar,%3C%20000%20is%20flow%20division.&text=The%20second%20element%20splits%20the,8%20streams%2C%20and%20so%20on.>
- Duer.M.(2011). Passive Mixing Systems Improve Storage Tank Water Quality. *Opflow*, 37(8),20-23.
- Shah.M.(2014) *Process Engineering: Agitation and Mixing*. Dharmsinh Desai University, India 164p. <https://www.dduanchor.org/site/wp-content/uploads/2014/11/Process-Engineering-Agitation-Mixing.pdf>
- Gates, L, E & Henley, T, L. (1985). *Liquid Agitation*. McGraw-Hill, Inc, New York, N.Y., U.S. 92p. <https://www.chemineer.com/chemineer-rep-documents/technical-articles/70-liquid-agitation/file.html>

Thermopedia. (2011). Agitation Devices. Retrieved 23, July, 2020, from [AGITATION DEVICES \(thermopedia.com\)](http://thermopedia.com/AGITATION_DEVICES)

Lytra, M. (2019). *Hydrolics of Lamilla Sedimentation*. Master's thesis, Division of Water Resources Engineering Department of Building & Environmental Technology Lund University, Lund, Sweden.

<https://lup.lub.lu.se/luur/download?func=downloadFile&recordOid=8991326&fileOid=8991327>

Binnie, C. & Kimber, M. & Smethurst, G. *Basic Water Treatment (3rd ed.)*. IWA Publishing, London, U.K.

Caputo, F. (2015) *Measuring Zeta Potential*. Research Report. European Nanomedicine Characterisation Laboratory. 19p. <http://www.euncl.eu/about-us/assay-cascade/PDFs/Prescreening/EUNCL-PCC-002.pdf?m=1468937877&#:~:text=During%20a%20zeta%20potential%20measurement,measured%20by%20a%20Doppler%20interferometer>.

West, A. (2018). *Self-Assembly Processes at Interfaces*. *Science Direct*, from <https://www.sciencedirect.com/topics/physics-and-astronomy/streaming-potential>

Fondriest Environmental Learning Center. *Turbidity, Total Suspended Solids & Water Clarity*. Retrieved 30 June, 2020, from <https://www.fondriest.com/environmental-measurements/parameters/water-quality/turbidity-total-suspended-solids-water-clarity/>

Horner, R.M.W. & Jarvis, R.J. & Mackie, R.I. (1986). *Deep Bed Filtration: A New Look at the Basic Equations*, Department of Civil Engineering and Department of Mathematical Sciences, the University of Dundee DDI HN, Scotland. <https://www.sciencedirect.com/science/article/pii/0043135486900114>

Tutorialspoint. (2019). *Control System*. Retrieved 24 June, 2020 from https://www.tutorialspoint.com/control_system/index.asp

Ma,S.C. (2012). *Design of a lab-scale direct-filtration system and Its Application in Process Lab*. Master's thesis. Michigan Technological University, Michigan, U.S.

Shulei Li.&Lihui Gao. &Yijun Cao. &Xiahui Gui. &Zhen Li. (2016) *Effect of pH on the flocculation behaviours of kaolin using a pH-sensitive copolymer*. (pp. 729-737). IWA Publishing, Longdon, U.K.

Kirikkaya, E.B. &Basaran, B. (2019). *Investigation of the Effect of the Integration of Arduino to Electrical Experiments on Students' Attitudes towards Technology and ICT by the Mixed Method*. European Journal of Educational Research. 48p.
https://www.researchgate.net/publication/330424867_Investigation_of_the_Effect_of_the_Integration_of_Arduino_to_Electrical_Experiments_on_Students'_Attitudes_towards_Technology_and_ICT_by_the_Mixed_Method

Britannica(2018). *Water Purification*. Retrieved 22 July, 2020, from <https://www.britannica.com/topic/water-purification>.

Appendix A Arduino Code Programs

A1 Motor Control Code for the Water Pump

```
float potPen=A0; // set Pin A0 as the value reader

float Voltage; // voltage to be measured
float readValue; // the value read by potPen
void setup()
{
  pinMode(potPen, INPUT); // set potPen as Input
  Serial.begin(9600);
}

void loop()
{
  readValue=analogRead(potPen); // get the value read by potPen
  Voltage=readValue*5/1023*2; // calculate voltage from value
  Serial.println(Voltage); // print voltage
  delay(1000);
}
```

A2 Turbidity Sensor Calibration Code

```
int turbidityPin=A0;
//int voltControl=3;
void setup() {
  // put your setup code here, to run once:
  Serial.begin(9600);
  pinMode(turbidityPin, INPUT);
  //pinMode(voltControl, 3);
}

void loop() {
  // put your main code here, to run repeatedly:
  //analogWrite(voltControl, 230);
  int value=analogRead(turbidityPin);
  float volt=value*(5.0/1024.0);
  float NTU=-1120.4*volt*volt+5742.3*volt-4352.9;
  Serial.println(NTU);
  delay(1000);
}
```

A3 PH Sensor Calibration Code

```
float calibration = 0; //change this value to calibrate
const int analogInPin = A1;
int sensorValue = 0;
unsigned long int avgValue;
float b;
int buf[10],temp;
void setup() {
  Serial.begin(9600);
}

void loop() {
  for(int i=0;i<10;i++)
  {
    buf[i]=analogRead(analogInPin);
    delay(30);
  }
  for(int i=0;i<9;i++)
  {
    for(int j=i+1;j<10;j++)
    {
      if(buf[i]>buf[j])
      {
        temp=buf[i];
        buf[i]=buf[j];
        buf[j]=temp;
      }
    }
  }
  avgValue=0;
  for(int i=2;i<8;i++)
  avgValue+=buf[i];
  float pHVol=(float)avgValue*5.0/1024/6;
  float pHValue = -5.70 * pHVol;
  Serial.print("sensor = ");
  pHValue=pHValue*(-1) + calibration;
  Serial.println(pHVol);
  pHValue=2.3166*pHVol+2.03;
  Serial.println(pHValue);
  delay(2500);
}
```

A4 Dosing Pump Testing Code

```
#include <Servo.h>

Servo myservo;

#define PUMPPIN A0 //peristaltic pump control pin, connect to arduino digital pin 9
#define waitTime 2000 //interval time(ms) between every state

void setup()
{
  myservo.attach(PUMPPIN);
}

void loop()
{
  //myservo.write(0); //Clockwise maximum speed rotation
  //delay(waitTime);
  //myservo.write(90); //Stop
  //delay(waitTime);
  myservo.write(175); //Counterclockwise maximum speed rotation
  //delay(waitTime);
  //myservo.write(90); //Stop
  //delay(waitTime);
}
```

A5 Flowmeter Testing Code

```
volatile int flow_frequency; // Measures flow sensor pulses
unsigned int l_hour; // Calculated litres/hour
unsigned char flowsensor = 7; // Sensor Input
unsigned long currentTime;
unsigned long cloopTime;
void flow () // Interrupt function
{
  flow_frequency++;
}
void setup()
{
  pinMode(flowsensor, INPUT);
  digitalWrite(flowsensor, HIGH); // Optional Internal Pull-Up
  Serial.begin(9600);
  attachInterrupt(0, flow, RISING); // Setup Interrupt
  sei(); // Enable interrupts
  currentTime = millis();
  cloopTime = currentTime;
}
void loop ()
{
  currentTime = millis();
  // Every second, calculate and print litres/hour
  if(currentTime >= (cloopTime + 1000))
  {
    cloopTime = currentTime; // Updates cloopTime
    // Pulse frequency (Hz) = 7.5Q, Q is flow rate in L/min.
    l_hour = (flow_frequency * 60 / 7.5); // (Pulse frequency x 60 min) / 7.5Q = flowrate in L/hour
    flow_frequency = 0; // Reset Counter
    Serial.print(l_hour, DEC); // Print litres/hour
    Serial.println(" L/hour");
  }
}
```

Final Code

```
#include <Servo.h>

Servo myservo;

#define PUMPPIN 19

int turbidityPinOne=A11;

int turbidityPinTwo=A12;

// zeta potential

int zetaPin=A0;

float calibration = 0; //change this value to calibrate

const int pHPinOne = A8;

const int pHPinTwo=A1;

int sensorValue = 0;

unsigned long int avgValue;

float b;

int buf[10],temp;

volatile int flow_frequency; // Measures flow sensor pulses

float l_hour; // Calculated litres/hour
```

```
float l_min;

unsigned char flowsensor = 2; // Sensor Input

unsigned long currentTime;

unsigned long cloopTime;

int divider=4; // divider to adjust the flowrate according to the time delay
```

```
void flow () // Interrupt function
```

```
{
```

```
    flow_frequency++;
```

```
}
```

```
void setup() {
```

```
    // for turbidities
```

```
    Serial.begin(9600);
```

```
    pinMode(turbidityPinOne,INPUT);
```

```
    pinMode(turbidityPinTwo,INPUT);
```

```
    //pinMode(voltControl,3);
```

```
    float adju;
```

```
pinMode(flowsensor, INPUT);

digitalWrite(flowsensor, HIGH); // Optional Internal Pull-Up

Serial.begin(9600);

attachInterrupt(0, flow, RISING); // Setup Interrupt

sei(); // Enable interrupts

currentTime = millis();

loopTime = currentTime;

//attach the dosing pin numbers to the dosing pumps

myservo.attach(PUMPPIN);

//zeta potential

pinMode(zetaPin,INPUT);

}

void loop() {

myservo.write(180);

// for zeta potential

float zetaPotential=analogRead(zetaPin);

float voltage= zetaPotential * (5.0 / 1023.0);
```

```

Serial.print("Zeta Potential: ");

Serial.println(voltage);

// for turbidities

int valueOne=analogRead(turbidityPinOne);

float voltOne=valueOne*(5.0/1024.0);

int valueTwo=analogRead(turbidityPinTwo);

float voltTwo=valueTwo*(5.0/1024.0);

float NTUOne=3042*voltOne*voltOne-17546*voltOne+15238.67;

//NTUOne=-900*voltOne+3645;

NTUOne=-628*voltOne+2438;

float NTUTwo=794*voltTwo*voltTwo-6936*voltTwo+15238.67;

//NTU=NTU-1000;

//NTUTwo=-846*voltTwo+3080;

//NTUTwo=-573*voltTwo+2827;

NTUTwo=-628*voltTwo+2438;

Serial.print("turbidity voltage 1: ");

Serial.println(voltOne);

Serial.print("turbidity 1 :");

Serial.println(NTUOne);

```

```
Serial.print("turbidity voltage 2: ");
```

```
Serial.println(voltTwo);
```

```
Serial.print("turbidity 2: ");
```

```
Serial.println(NTUTwo);
```

```
// for pH sensor One
```

```
for(int i=0;i<10;i++)
```

```
{
```

```
buf[i]=analogRead(pHPinOne);
```

```
delay(30);
```

```
}
```

```
for(int i=0;i<9;i++)
```

```
{
```

```
for(int j=i+1;j<10;j++)
```

```
{
```

```
if(buf[i]>buf[j])
```

```
{
```

```
temp=buf[i];
```

```
buf[i]=buf[j];
```

```
buf[j]=temp;
```

```
}
```

```

}

}

avgValue=0;

for(int i=2;i<8;i++)

avgValue+=buf[i];

float pHVol=(float)avgValue*5.0/1024/6;

float phValueOne = -5.70 * pHVol;

Serial.print("sensor = ");

phValueOne=phValueOne*(-1) + calibration;

Serial.println(pHVol);

//phValue=3.7*pHVol-0.59;

phValueOne=2.069*pHVol+2.675862;

Serial.print("pH before settling: ");

Serial.println(phValueOne);

// for pH sensor Two

for(int i=0;i<10;i++)

{

buf[i]=analogRead(pHPinTwo);

```

```

delay(30);

}

for(int i=0;i<9;i++)

{

for(int j=i+1;j<10;j++)

{

if(buf[i]>buf[j])

{

temp=buf[i];

buf[i]=buf[j];

buf[j]=temp;

}

}

}

avgValue=0;

for(int i=2;i<8;i++)

avgValue+=buf[i];

float pHVol2=(float)avgValue*5.0/1024/6;

float pHValueTwo = -5.70 * pHVol2;

Serial.print("sensor = ");

pHValueTwo=pHValueTwo*(-1) + calibration;

```

```

Serial.println(pHVol2);

//phValue=3.7*pHVol-0.59;

//phValueTwo=3.4*pHVol2-0.02;

phValueTwo=2.7273*pHVol2+1.49;

Serial.print("pH after settling: ");

Serial.println(phValueTwo);

// flowrate meter

currentTime = millis();

// Every second, calculate and print litres/hour

if(currentTime >= (cloopTime + 1000))

{

    cloopTime = currentTime; // Updates cloopTime

    // Pulse frequency (Hz) = 7.5Q, Q is flow rate in L/min.

    l_min = (flow_frequency / 6.9); // (Pulse frequency x 60 min) / 7.5Q = flowrate in
L/hour

    //l_min=l_hour/60;

    l_min=l_min/divider;

    flow_frequency = 0; // Reset Counter

    /* if(l_min!=0)

    { */

```

```
//myservo.write(180);

/* }

else

{

myservo.write(90);

} */

Serial.print(l_min, DEC); // Print litres/hour

Serial.println(" L/min");

}

Serial.println();

delay(divider*1000);

}
```